NASA TECHNICAL MEMORANDUM

NASA TM X-2362

NASA TM X-2362

INVESTIGATION OF SLOSH ANOMALY IN APOLLO LUNAR MODULE PROPELLANT GAGE

by Harland F. Scholl, Larry D. Pinson, and David G. Stephens

Langley Research Center
Hampton, Va. 23365

NATIONAL AERONAUTICS AND SPACE ADMINISTRATION • WASHINGTON, D. C. • OCTOBER 1971

1. Report No. NASA TM X-2362	2. Government Accession No.	3. Recipient's Catalog No.
4. Title and Subtitle INVESTIGATION OF SLOSH ANOMALY IN APOLLO LUNAR MODULE PROPELLANT GAGE		5. Report Date October 1971 6. Performing Organization Code
7. Author(s) Harland F. Scholl, Larry D. Pinson, and David G. Stephens		8. Performing Organization Report No. L-7757
9. Performing Organization Name and Address NASA Langley Research Center Hampton, Va. 23365		10. Work Unit No. 114-08-13-03 11. Contract or Grant No.
12. Sponsoring Agency Name and Address National Aeronautics and Space Administration Washington, D.C. 20546		13. Type of Report and Period Covered Technical Memorandum 14. Sponsoring Agency Code

15. Supplementary Notes

Technical Film Supplement L-1088 available on request.

16. Abstract

An experimental and analytical program was conducted to identify a liquid slosh phenomenon in the Apollo lunar module (LM) which resulted in a 30- to 45-second premature indication of a low level of propellant from the propellant quantity gage system (PQGS) in the LM descent propulsion system. This research was conducted to determine the corrective action required to minimize spurious effects due to the interaction of the liquid and gage and to extrapolate laboratory results to LM flight conditions. Developed and qualified were a fixed cylindrical baffle and modified PQGS tube which suppressed the oscillatory motion of the liquid in the tank and reduced the PQGS premature low-level indicator penalty to less than 5 seconds. Preliminary flight data from Apollo 14 indicate that the device operated successfully.

17. Key Words (Suggested by Author(s))	18. Distribution Statement
Lunar module Propellant gage Slosh	Unclassified – Unlimited

19. Security Classif. (of this report)	20. Security Classif. (of this page)	21. No. of Pages	22. Price*
Unclassified	Unclassified	39	$3.00

*For sale by the National Technical Information Service, Springfield, Virginia 22151

INVESTIGATION OF SLOSH ANOMALY IN APOLLO LUNAR MODULE PROPELLANT GAGE

By Harland F. Scholl, Larry D. Pinson,
and David G. Stephens
Langley Research Center

SUMMARY

As part of a program to better understand and possibly eliminate a premature indication of a low level of propellant which occurred in the descent propulsion system during the terminal lunar module (LM) landing maneuver on both Apollo 11 and 12 flights, experiments and analyses were undertaken to identify dynamic interaction between LM slosh and the propellant quantity gage system (PQGS) and to determine corrective action to minimize spurious effects due to this interaction. This report presents results of laboratory tests with model LM tanks fitted with various PQGS models, candidate baffle configurations, and simulated propellants. Test results were correlated with an analysis of the propellant-slosh-induced phenomena to better understand the behavior of the liquid in the PQGS under dynamic conditions and to examine the important similitude relationships required for extrapolating laboratory results to LM flight conditions.

Liquid slosh in both antisymmetric and symmetric modes within the tank causes relatively large fluctuations about a displaced mean level in the PQGS tube under steady-state vibratory excitation or under the transient input which could exist in the terminal phase of the LM landing. The mean level in the PQGS tube is also affected by the slosh amplitude and may be different than the average level in the tank. Results from Apollo 11 and 12 flights indicated a measurement error equivalent to approximately 30 to 45 seconds of flight time. The slosh-induced fluctuations within the PQGS have components at both the slosh frequency and twice the slosh frequency. The relative magnitudes depend upon the number and orientation of vent holes built into the gage tube. The magnitude and character of the induced fluctuations within the PQGS for low slosh amplitudes can be predicted by analysis.

Fluctuations within the PQGS were significantly reduced by decreasing the size of the PQGS tube vent holes; however, the error in mean level of the liquid within the tube remained virtually unchanged with this modification. A fixed cylindrical baffle (which can be installed through the PQGS port) was subsequently developed to suppress the oscillatory motion of the liquid in the tank and at the same time to reduce the mean level condition at

the nominal 25-cm liquid depth level (i.e., 5.6 percent fuel remaining). With the combination of modified PQGS and cylindrical baffle, the error in the low-level indicator was reduced to less than 5 seconds. Preliminary flight data from Apollo 14 indicate that the device operated successfully.

INTRODUCTION

Postflight analyses of the propellant utilization during the lunar module (LM) descent to touchdown of both Apollo 11 and 12 suggested that the propellant low-level alarm indicator was prematurely activated and therefore gave erroneous information on the amount of propellant remaining in the tanks. Each of the four LM descent propellant tanks is equipped with a propellant quantity gage system (PQGS), shown schematically in figure 1,

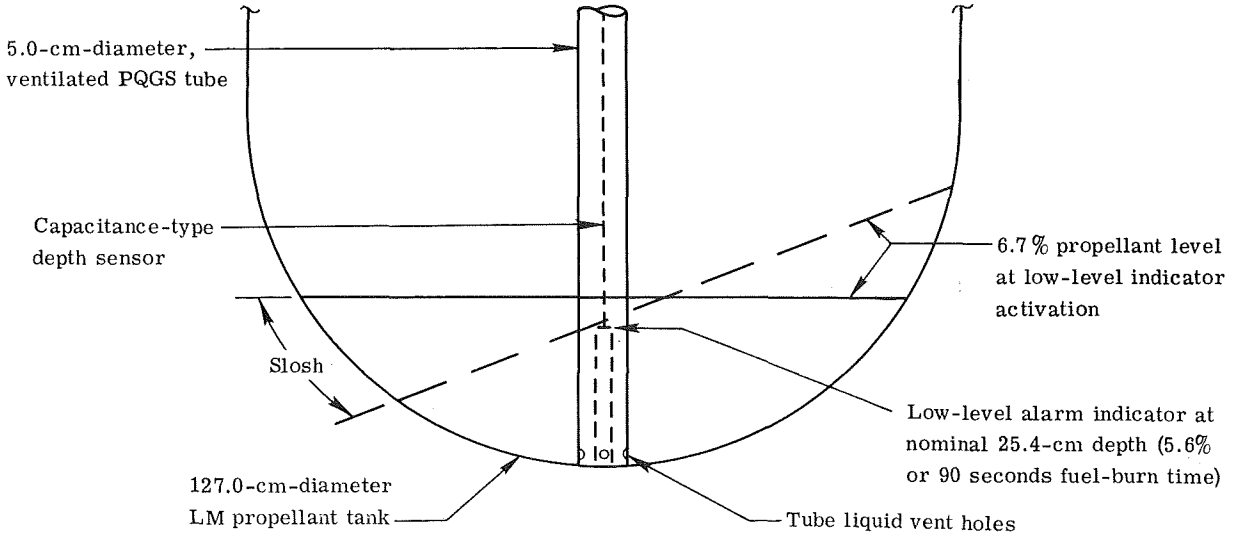

Figure 1.- Schematic of LM propellant quantity gage system (PQGS).

which monitors the depth of liquid within the tank and activates the low-level alarm. The PQGS consists of a nominal 5.0-cm-diameter ventilated tube located along the longitudinal axis of the tank and containing a capacitance-type depth sensor and a discrete low-level alarm indicator. When the liquid level in any of the PQGS tubes becomes less than 25 cm (5.6 percent propellant quantity or nominally 90 seconds of fuel-burn time remaining), a warning light, part of the low-level alarm indicator, is activated on the LM control panel. This light continues to burn even though the alarm sensor may have been only momentarily exposed. On both Apollo 11 and 12 the postflight calculations indicated that the light was prematurely activated; that is, the 90-second light was activated while propellant was available for approximately 120 seconds or more of flight. It was postulated that propellant slosh produced fluctuations of the liquid level in the PQGS tube of sufficient magnitude to cause this premature (30- to 45-second) low-level indication.

As a result of the anomalous behavior of the PQGS, the Langley Research Center, at the request of the Manned Spacecraft Center, initiated a program to better understand the behavior of the LM PQGS under dynamic conditions and, if possible, to determine corrective action. The program consisted of three phases: (1) Analyses and low-level sinusoidal slosh tests were conducted with model PQGS tubes. The purpose of this phase was to understand the mechanism by which the PQGS liquid level was altered dynamically and to screen several possibilities for correction. (2) Tests with detailed PQGS models and baffles were conducted with apparatus designed to simulate dynamic inputs from the reaction control system (RCS) of the LM. Test amplitudes were chosen up to the levels of slosh that were necessary to simulate the most severe conditions which could result from RCS translational inputs. This same apparatus was subsequently used to flight-qualify the modified PQGS which was installed in the LM tanks. (3) Simultaneously with the second phase, similitude studies were conducted to aid in formulating the test procedures and in extrapolating the results to flight conditions.

Electronic and software corrections were considered under a separate program, which was conducted by the LM prime contractor and the Manned Spacecraft Center.

The purpose of this report is to present highlights of the Langley portion of the LM PQGS anomaly study. Some results also are recorded in a 16-mm, silent, color film (L-1088) which is available for loan upon request from the Langley Research Center. A request card and a description of the film are included at the back of this document.

SYMBOLS

A_o	area of orifices, cm^2
A_p	cross-sectional area of PQGS tube, cm^2
C	damping constant, cm^{-1}
C_D	orifice discharge coefficient
C_1	ratio of area at vena contracta to area of orifice
C_p	ratio of dynamic pressure at PQGS tube to free-stream dynamic pressure
$C_{p,1}, C_{p,2}$	pressure coefficients for two portions of slosh cycle
g	acceleration due to earth gravity, cm/sec^2

h	quiescent liquid height, cm
h_o	liquid height outside of PQGS tube, cm
ℓ	characteristic length, cm
R	tank radius, cm
t	time, sec
u	surface displacement of liquid in PQGS tube, cm
V	liquid velocity, cm/sec
V_e	orifice-exit velocity, cm/sec
V_s	slosh velocity, cm/sec
x_o	maximum slosh amplitude, cm
δ	peak displacement of free liquid surface at tank center line, cm
θ	angle measured from free stream in direction of flow
μ	absolute viscosity, g/cm-sec
ν	kinematic viscosity, cm^2/sec
ρ	mass density of liquid, g/cm^3
σ	surface tension, N/m
ω_u	undamped natural frequency of liquid in PQGS tube, rad/sec
Ω	circular slosh frequency, rad/sec
ζ	fraction of critical damping

Subscripts:

M model

LM lunar module

A dot over a symbol represents derivative with respect to time.

APPARATUS

Tests were conducted with a clear acrylic plastic hemispherical tank, shown in figure 2, which had the same diameter (127.0 cm) as the LM descent propellant tank.

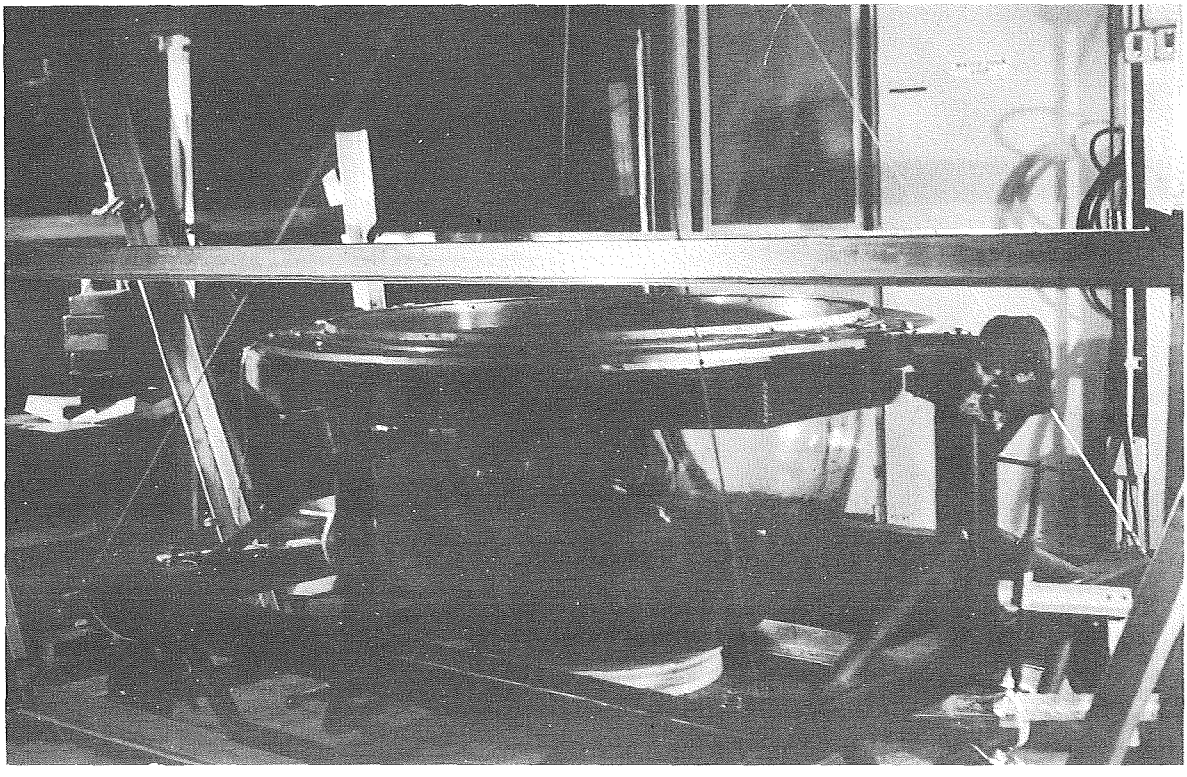

L-70-3976

Figure 2.- Full-scale (127.0 cm) acrylic plastic test tank in drop-weight apparatus.

Replica antivortex baffles (used in the LM tanks to suppress liquid vortex motion at low liquid depths) and a "zero-g can" (which trapped sufficient propellant for engine restart during zero-g flight), shown in figure 3, were attached at the proper location to the tank bottom. The tank was an integral part of the drop-weight slosh apparatus depicted schematically in figure 4. Use of this apparatus allowed the liquid in the tank to be excited manually in the antisymmetric slosh mode. Provisions were made for draining the tank

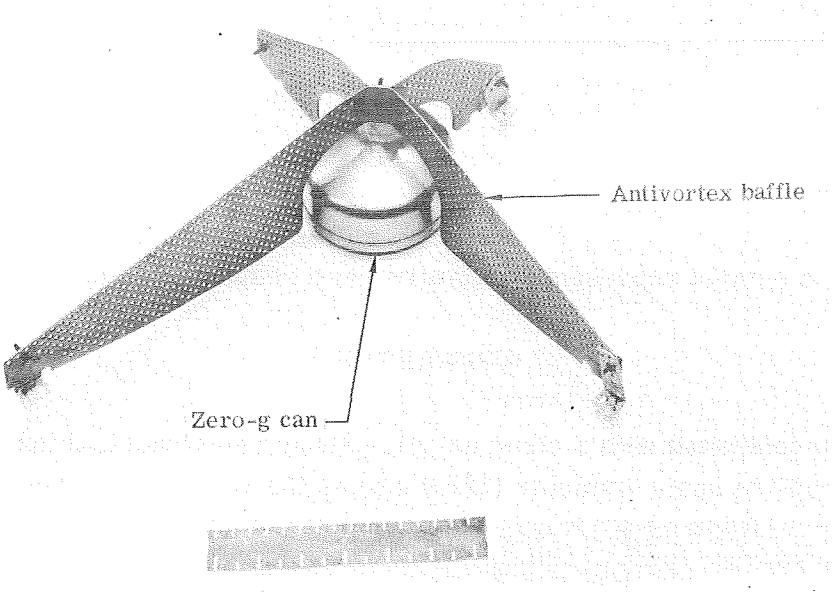

L-70-5749.1

Figure 3.- Antivortex baffle and zero-g can.

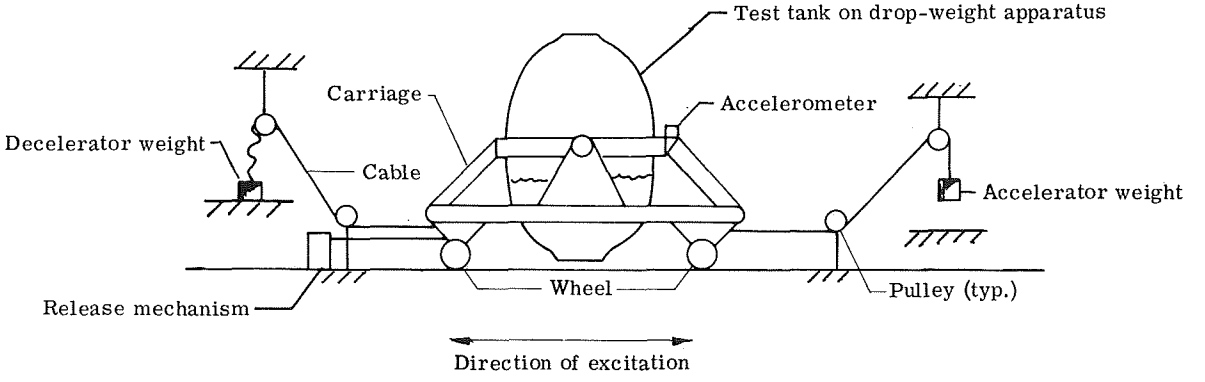

Figure 4.- Schematic of drop-weight slosh apparatus.

at a maximum flow rate of 0.23 m^3/min. Also, transient loads, which were designed to simulate translational inputs of the RCS, were imparted to the tank by means of a drop-weight cable system. Upon activation of the release mechanism the accelerator weight moved down, and thereby caused the carriage and tank to move horizontally. At a predetermined distance the accelerator weight was stopped, and the carriage entered a coast phase. After coasting for another predetermined distance, the carriage was slowed when the decelerator weight was lifted. When the carriage reached zero velocity, the transient input was considered to be terminated. An accelerometer mounted on the tank measured input acceleration levels. Liquid slosh amplitudes within the tank were sensed by a calibrated differential pressure transducer.

TEST SPECIMENS

Two transparent acrylic plastic PQGS tubes, shown in figure 5, were used for most of the tests. The tubes were 91.5 cm long and had a 5.0-cm outside diameter and a 0.3-cm

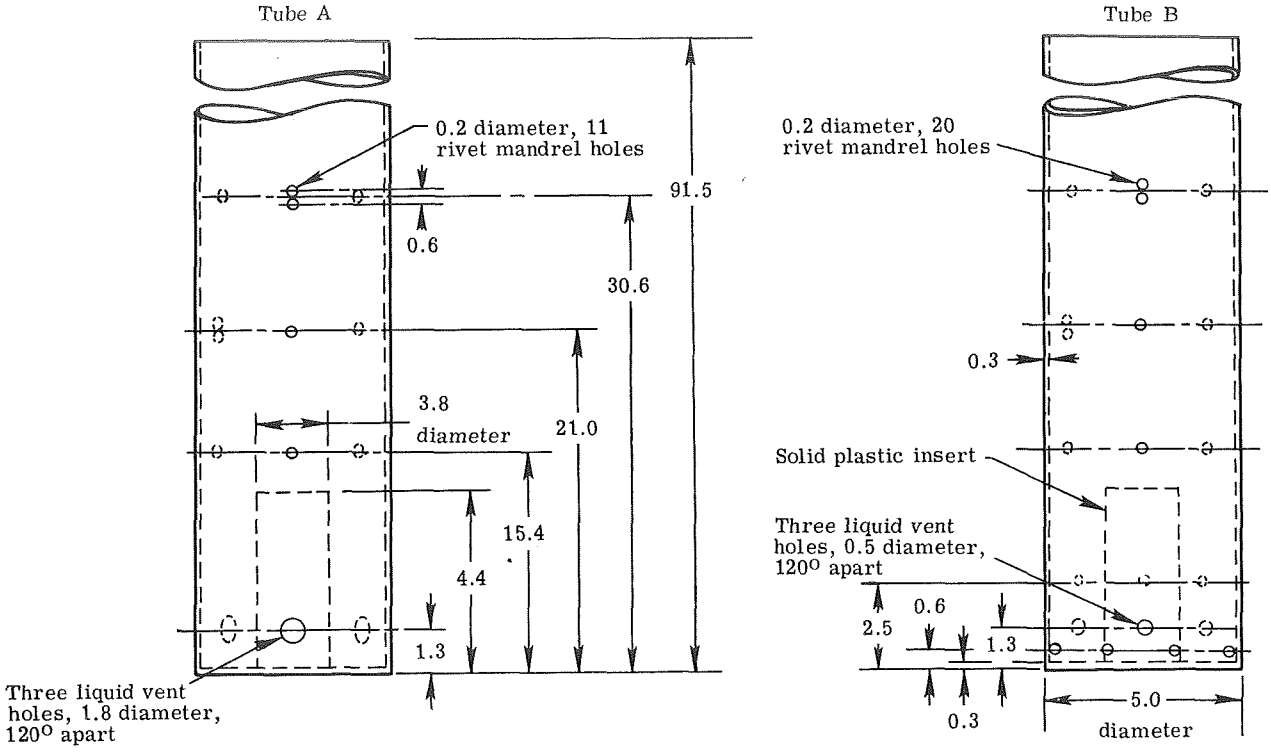

Figure 5.- Acrylic plastic PQGS tubes. Drawing is not to scale; all dimensions are in centimeters.

wall thickness. Each had a solid, clear plastic cylinder, 4.4 cm long and 3.8 cm in diameter, inserted in the base of the tube to represent the volume of electrical apparatus in the flight LM PQGS tube. Tube A was a near replica of the Apollo 11 and 12 design with eleven 0.2-cm-diameter holes, three at 15.4 cm, four at 21.0 cm, and four at a nominal 30.6 cm from the base of the tube. These holes were spaced and sized from preliminary information to represent rivet mandrel holes in the flight tube. In addition, tube A had three 1.8-cm-diameter holes, 120° apart, centered 1.3 cm from the base of the tube, to vent the liquid. For tube B, the vent holes were reduced to 0.5 cm in diameter to provide the minimum required liquid vent area based on steady-drain calculations. Also, nine additional rivet mandrel holes (0.2-cm diameter), six at 0.6 cm and three at 2.5 cm from the base, were added to tube B to more closely represent the pattern of rivet mandrel holes in the flight tube. Both tubes were fitted with a resistance-wire transducer system, which had an electrical output proportional to the instantaneous liquid height at the tube center line and thus monitored variations in the liquid surface within the tube. Combinations of PQGS tubes and slosh-suppression devices (in addition to the antivortex baffles) were tested in an effort to find the simplest correction to the anomaly.

Preliminary test phases involving other types of test apparatus and specimens were conducted in addition to the apparatus and specimens described herein. Although these preliminary tests did not actually identify or correct the PQGS problem, they were required in order to explore all possible problem areas and to support and verify the experimental procedure discussed herein. These phases are presented as appendixes to this paper.

TEST PROCEDURE

Steady-State Tests

The test program is summarized in table I. To investigate the response of the liquid in the PQGS tube over a wide range of slosh amplitudes (0 to 40.6 cm), all associated equipment was placed in the test tank, which was filled with water to a depth of either 12.7 or 25.4 cm. (Use of water as a test liquid is discussed in the section entitled "Scaling.") The apparatus was excited horizontally by hand at the frequency of the antisymmetric slosh mode until the desired slosh amplitude was attained. Data from the various sensors were recorded on an oscillograph. This procedure was repeated for both tubes.

Tests With Simulated Inputs From Reaction Control System (RCS)

To simulate the most severe tank translations which might be expected from flight control pulses of the LM reaction control system, the drop weights were adjusted at both ends of the apparatus to produce the desired acceleration time history (ref. 1). A quick-release mechanism was used to initiate free fall of the accelerator weight, which in turn drove the apparatus horizontally, as previously described. It should be noted that although the designed acceleration level was attained, the apparatus did not accurately reproduce the desired square-wave-shaped acceleration input. (See fig. 6.) Instead, the dwell time at the peak acceleration for the resulting wave was shorter than desired. However, the designed peak acceleration of 0.2g was estimated to exceed probable flight levels of the LM. It was believed that this greater acceleration level compensated for the shorter

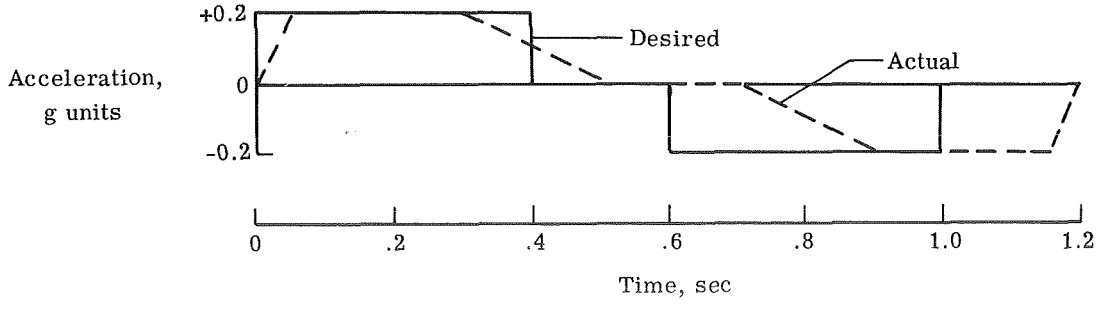

Figure 6.- Acceleration level of drop-weight slosh apparatus.

period of dwell at the peak acceleration. Peak slosh amplitudes of 38.1 to 40.6 cm resulted from these simulated RCS pulses. Measurements of tank motions, slosh amplitudes, and variations in the liquid surface inside the tube were recorded as oscillograms. This procedure was repeated for both PQGS tubes and all slosh-suppression devices tested.

ANALYSIS

The configuration and nomenclature used in the analysis are shown in figure 7. The quiescent depth of the liquid at the center line of the hemispherical tank is h. When the slosh reaches the maximum value x_o, the displacement of the free surface of the

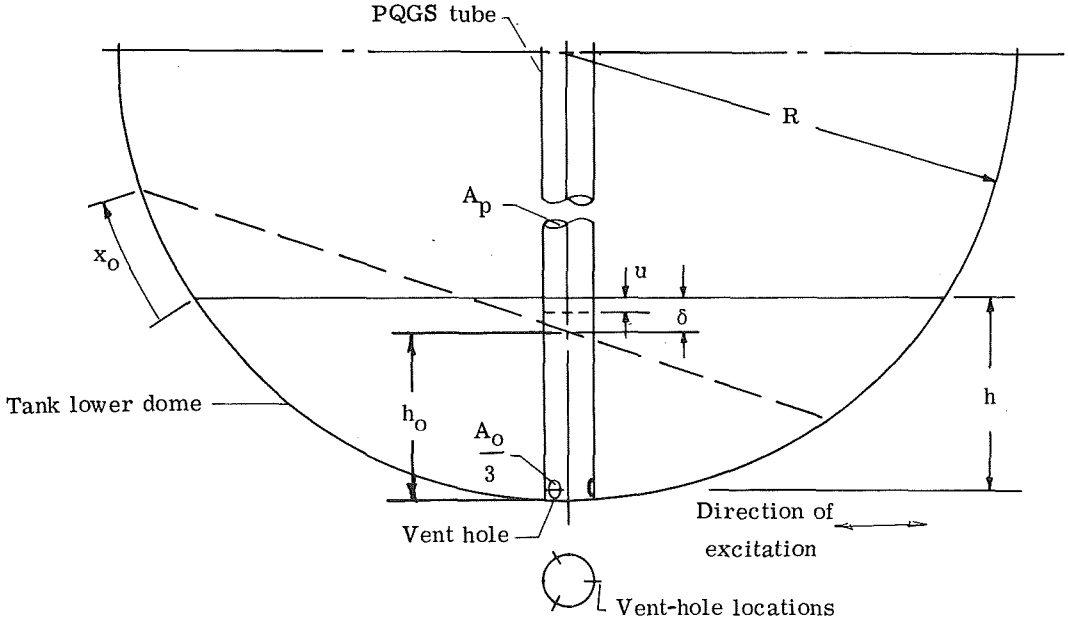

Figure 7.- Analytical model.

liquid from the quiescent location at the tank center line is δ. The variation of this surface displacement was assumed to occur harmonically at twice the slosh frequency. This displacement was calculated with the assumption that the surface of the liquid remains planar during slosh motion. In this analysis, the PQGS tube had three equally spaced circumferential vent holes, each with equal area $A_o/3$, located near the bottom in the PQGS tube wall. Changes in the level of the liquid outside the tube resulted in flow through the holes, which caused an additional surface displacement u within the tube.

Motion of liquid within the PQGS tube is described by an equation obtained by application of d'Alembert's principle and the equation of continuity. Two quantities affect the pressure outside the holes in the PQGS tube: the change in static pressure due to the

drop in liquid level at the center line of the tank and the dynamic pressure due to the slosh velocity V_s. The holes in the tube walls are assumed to act as orifices with discharge coefficient C_D equal to 0.6. Thus, if the exit velocity through the orifices is V_e, the continuity equation yields

$$V_e = \frac{1}{C_D}\frac{A_p}{A_o}\dot{u} \tag{1}$$

where A_p is the cross-sectional area of the PQGS tube, A_o is the total orifice area, and $\dot{u}$ is the time rate of change of the inside surface displacement u. Summation of forces at the plane of the vena contracta yields the following equation:

$$C_1 A_o\left[\rho g(h - u) - \rho h\ddot{u} - \frac{1}{2}\rho V_e^2\right] = C_1 A_o\left(\rho g h_o + C_p \frac{1}{2}\rho V_s^2\right) \tag{2}$$

where C_1 is the ratio of the area of the stream at the vena contracta to the orifice area, ρ is the mass density of the liquid, g is the acceleration due to gravity, h_o is the height of the liquid outside the PQGS tube, and C_p is a coefficient which relates the free-stream dynamic pressure due to the slosh velocity and the pressure outside the orifices which results from flow around the PQGS tube. The quantities ρ, C_1, and A_o all cancel in equation (2). Substituting for V_e from equation (1) and rearranging gives the equation of motion

$$\ddot{u} + C|\dot{u}|\dot{u} + \omega_u^2 u = \omega_u^2(h - h_o) - C_p \frac{\omega_u^2}{2g} V_s^2 \tag{3}$$

where

$$\omega_u = \sqrt{g/h}$$

and

$$C = \frac{\omega_u^2}{2gC_D^2}\left(\frac{A_p}{A_o}\right)^2$$

The absolute value signs were introduced to yield a force which opposes the motion regardless of the sign of the velocity. To obtain the right-hand side of equation (3) as an explicit function of time, the following relations were used (fig. 7):

$$h - h_o = (\delta/2)(1 + \cos 2\Omega t) \tag{4}$$

$$\delta = (R - h)\left[\sec\left(\frac{x_o}{R}\right) - 1\right] \tag{5}$$

$$V_s = -\Omega x_o \sin \Omega t \tag{6}$$

where Ω is the circular frequency of slosh and R is the radius of the tank. Substitution of equations (4), (5), and (6) into equation (3) yields

$$\ddot{u} + C|\dot{u}|\dot{u} + \omega_u{}^2 u = A + B \cos 2\Omega t \tag{7}$$

where

$$A = \frac{\omega_u{}^2 \delta}{2} - \frac{\omega_u{}^2 \Omega^2 x_o{}^2}{4g} C_p$$

and

$$B = \frac{\omega_u{}^2 \delta}{2} + \frac{\omega_u{}^2 \Omega^2 x_o{}^2}{4g} C_p$$

Thus, with the pressure coefficient, the slosh frequency, and the slosh amplitude assumed to be known, the response of the liquid surface inside the PQGS tube was calculated by solving equation (7). In this analysis, equation (7) was integrated numerically on a digital computer and was also solved by analog simulation for verification.

Hydrodynamic theory yields a pressure coefficient for flow past a cylinder that is independent of the sign of the flow velocity. (See ref. 2, p. 227.) Thus, for slosh in which the velocity is varying harmonically, C_p is a constant for a given placement of vent holes. This theory was used in generating preliminary results. However, consideration of viscous effects shows that for the three-hole arrangement, the pressure coefficient depends on the direction of flow around the PQGS tube. Thus, different pressure coefficients result, depending upon the sign of the slosh velocity. In this analysis pressure coefficients were obtained from figure 8, which is reproduced from reference 3. The figure shows the variation of pressure coefficient with angular position θ, where θ is the angle measured from the free stream with the origin on the upstream side of the cylinder. Separate curves result for different values of the Reynolds number. In the present analysis the velocity used in calculating the Reynolds number to obtain the pressure coefficient was the root-mean-square value of the slosh velocity. As seen in figure 8, the change in pressure coefficients with moderate changes in Reynolds number is small, and for Reynolds numbers above 25 000, the change in pressure coefficient is negligible.

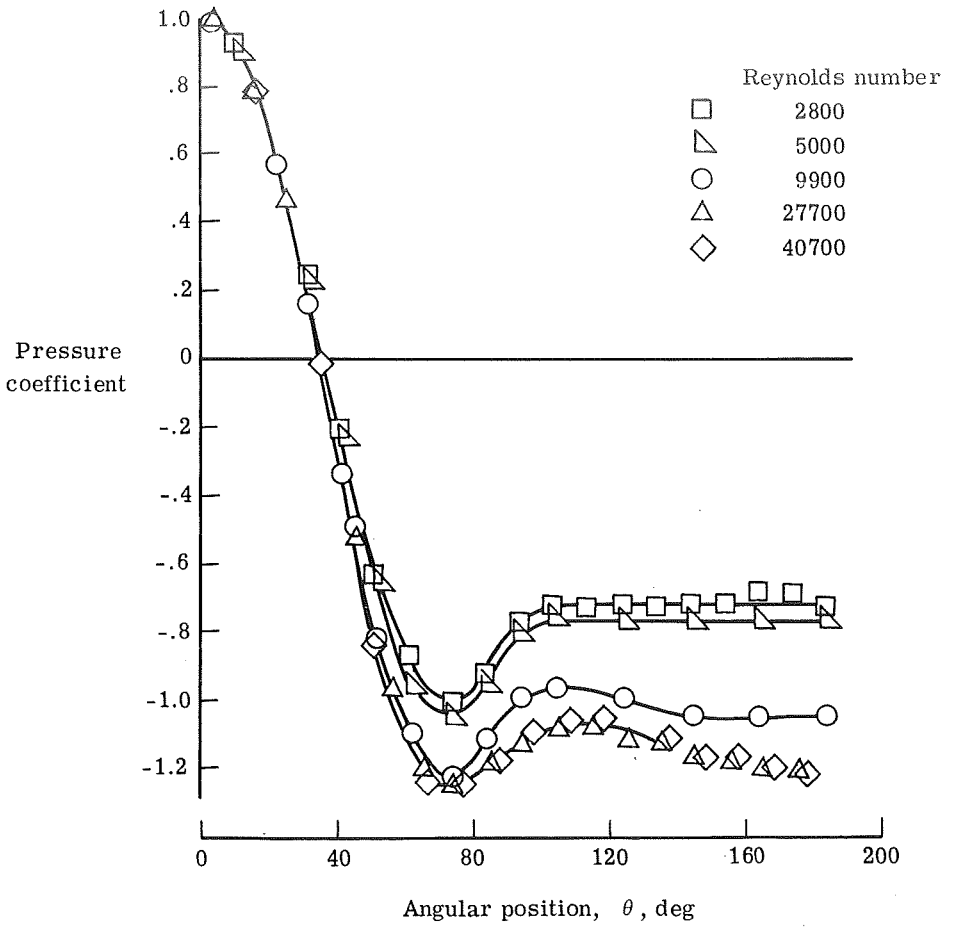

Figure 8.- Pressure coefficients associated with a cylinder in a free stream.

To obtain an insight into the external-flow directional effect, the right-hand side of equation (7) was expanded into a Fourier series incorporating the change in pressure coefficient with the sign of the slosh velocity. The pressure coefficient was assumed to take the values $C_{p,1}$ and $C_{p,2}$ for the two portions of the slosh cycle. The result is

$$A + B\cos 2\Omega t = \left[\frac{\omega_u^2\delta}{2} + \frac{\omega_u^2\Omega^2 x_o^2}{8g}\left(C_{p,1} + C_{p,2}\right)\right] + \left[\frac{\omega_u^2\delta}{2} - \frac{\omega_u^2\Omega^2 x_o^2}{8g}\left(C_{p,1} + C_{p,2}\right)\right]\cos 2\Omega t$$

$$+ \sum_{n=1,3,5\ldots}^{\infty} \frac{\omega_u^2\Omega^2 x_o^2}{\pi g}\left(C_{p,2} - C_{p,1}\right)(-1)^n \frac{2 - n^2}{n(4 - n^2)}\cos n\Omega t \qquad (8)$$

The first term of the summation in equation (8) shows that when the external-flow directional effect is considered, a component of excitation occurs at the slosh frequency in addition to that which occurs at twice the slosh frequency. The significance of this

effect is demonstrated in figure 9, which shows time histories for both excitation and response obtained from the analog simulation. In figure 9(a) the external-flow directional effect is omitted, and both the response and excitation occur at a frequency which is twice the slosh frequency. When the directional effect is included (fig. 9(b)), the excitation becomes distorted, but the frequency is the slosh frequency. The response is also at the slosh frequency. Thus, the character of the calculated response of the liquid surface inside the PQGS tube is drastically altered by inclusion of the directional effect. The results of the analysis, which are presented in appendix A in comparison with experiment, therefore, include this effect.

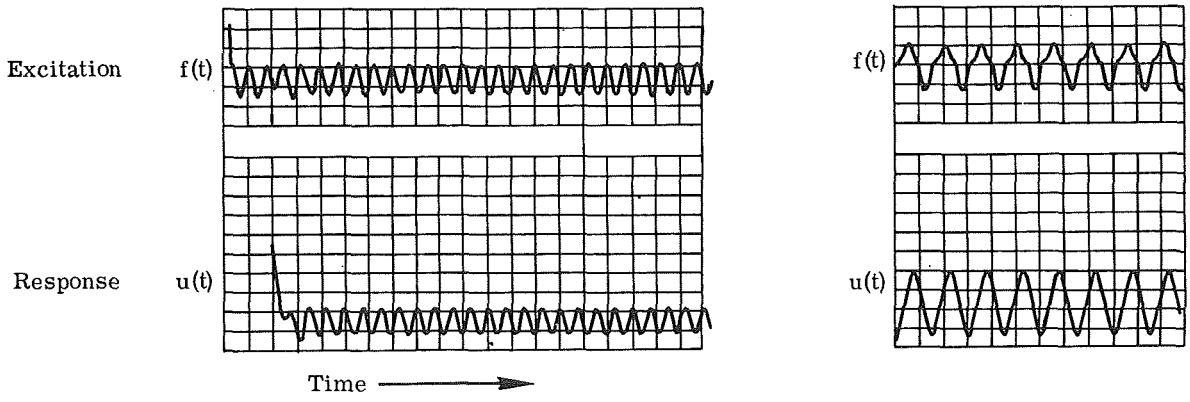

(Scale is same for both (a) and (b).)

(a) External-flow directional effect omitted.

(b) External-flow directional effect included.

Figure 9.- Typical tank excitation and PQGS response time histories showing external-flow directional effect.

SCALING

Several candidate liquids were investigated for the PQGS test program in an effort to simulate the propellant properties applicable to LM flight conditions. The properties considered and their representation by three candidate liquids are discussed in this section. Results are also presented on the effect on overall system damping of using various liquids.

Involved in liquid dynamics are inertial, viscous, and gravitational forces, which depend upon liquid density, viscosity, local gravitational field, and surface tension. For dynamic similitude, it is important that the relationship between the forces in equation (7) remains the same in both the laboratory models and the flight condition. Six nondimensional parameters can be formulated:

Parametric designation	Force ratio
Froude number	$\frac{\text{Inertial}}{\text{Gravitational}} \doteq \frac{V^2}{gl}$
Reynolds number	$\frac{\text{Inertial}}{\text{Viscous}} \doteq \frac{\rho V l}{\mu}$
Galileo number	$\frac{\text{Gravitational}}{\text{Viscous}} \doteq \frac{gl^3}{\nu^2}$
Weber number	$\frac{\text{Inertial}}{\text{Surface tension}} \doteq \frac{\rho V^2 l}{\sigma}$
Ohnesorge number	$\frac{\text{Viscous}}{\text{Surface tension}} \doteq \frac{\mu}{(\rho l \sigma)^{1/2}}$
Bond number, B_o	$\frac{\text{Gravitational}}{\text{Surface tension}} \doteq \frac{\rho g l^2}{\sigma}$

To examine the importance of surface tension for the LM conditions, the Bond number was calculated as follows for the PQGS tube and the LM tank configurations for the propellant N_2O_4 and Aerozine-50 under conditions of lunar gravity:

	N_2O_4	Aerozine-50
Tube	222	124
Tank	139 000	78 000

The resulting values $(B_o > 100)$ suggested that surface tension would have a negligible effect. (See ref. 4.) Therefore, the phenomena of interest should be insensitive to Weber, Bond, and Ohnesorge numbers. The parameters most pertinent to the investigation were considered to be Froude, Reynolds, and Galileo numbers.

Since the experiment was done on earth with a full-size tank and the natural frequencies ω are proportional to $\sqrt{g}$, then $V = \omega l = l\sqrt{g}$ and

Froude number ratio	$\frac{\text{LM}}{\text{Model}} = 1$
Reynolds number ratio	$\frac{\text{LM}}{\text{Model}} = 0.408 \frac{\nu_M}{\nu_{LM}}$
Galileo number ratio	$\frac{\text{LM}}{\text{Model}} = 0.167\left(\frac{\nu_M}{\nu_{LM}}\right)^2$

Both the Reynolds number and the Galileo number could be made to equal the LM flight values by selecting liquids of appropriate viscosity as follows:

Ratio of LM/Model for –	Fuel (ν = 0.00865 cm^2/sec)			Oxidizer (ν = 0.00292 cm^2/sec)		
	Aerozine-50	Water (ν = 0.010 cm^2/sec)	Water + 25% sugar by weight (ν = 0.022 cm^2/sec)	N_2O_4	Water	Methyl alcohol (ν = 0.00745 cm^2/sec)
Reynolds number	0.408	0.470	1	0.408	1.39	1.04
Galileo number	.167	.221	1	.167	1.94	1.08
Froude number	1	1	1	1	1	1

The Froude, Reynolds, and Galileo numbers can be made approximately the same for the model and for full size if methyl alcohol is used in the model to represent the oxidizer (N_2O_4) and a sugar-water solution (sucrose) is used in the model to represent the fuel. To determine the suitability of water, which was considered to be a more desirable simulant because of its ease of handling and availability, tests were conducted in which overall system damping was evaluated for the three simulants just described. In considering the total system damping, at least three mechanisms are present, that is, tank damping due to boundary-layer losses (smooth-wall damping), damping due to antivortex baffles, and tube damping due to discharge coefficient C_D. As discussed in reference 5, smooth-wall damping is governed by Galileo number, whereas baffle damping (refs. 4 and 6) is dependent only upon geometry (Froude number). Discharge coefficient C_D depends upon Reynolds number.

The results of the tests for overall system damping are presented in figure 10. The figure is a plot of system decrement as a function of slosh amplitude for the three test liquids at the 25.4-cm depth. The figure shows that the overall system damping is virtually independent of the choice of liquid. In addition, slosh tests which were conducted with other PQGS tubes in tanks which contained alcohol and sucrose showed that the change in

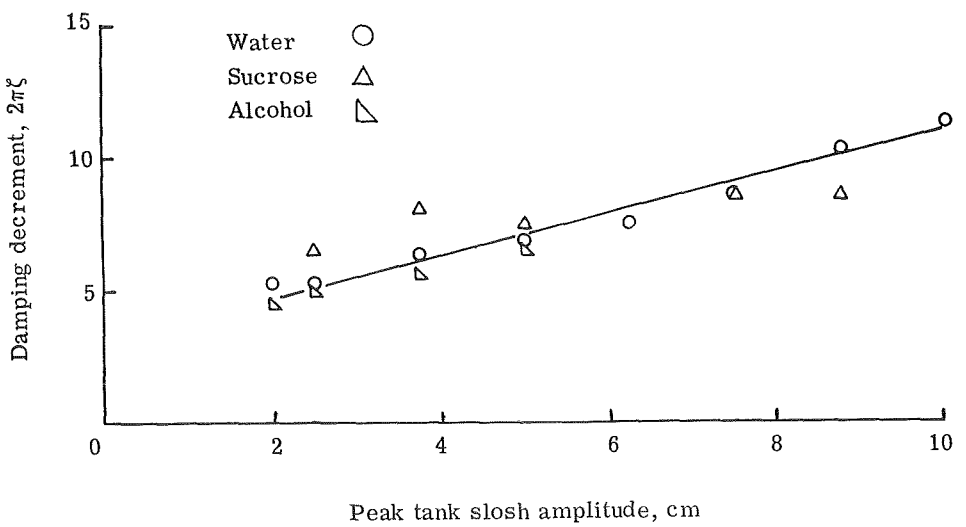

Figure 10.- Antisymmetric-mode damping in LM tank for several liquids at 25.4-cm depth.

kinematic viscosity, and hence Reynolds and Galileo numbers, had no substantial effect on the PQGS response. The results of both these tests led to the selection of water as the fuel simulant in all subsequent tests.

DISCUSSION AND RESULTS

Initial studies with the apparatus described in appendix A were conducted at low slosh amplitudes to provide insight into the basic liquid dynamics system. The results of these tests were compared with the analysis to gain assurance that all major effects were understood and accounted for. The comparison is presented in appendix A. With the assurance gained in the low-amplitude tests, studies with more detailed tubes were conducted with the higher slosh amplitudes which were possible in flight. As shown in figure 11 and verified both analytically and experimentally, the response in the PQGS tube

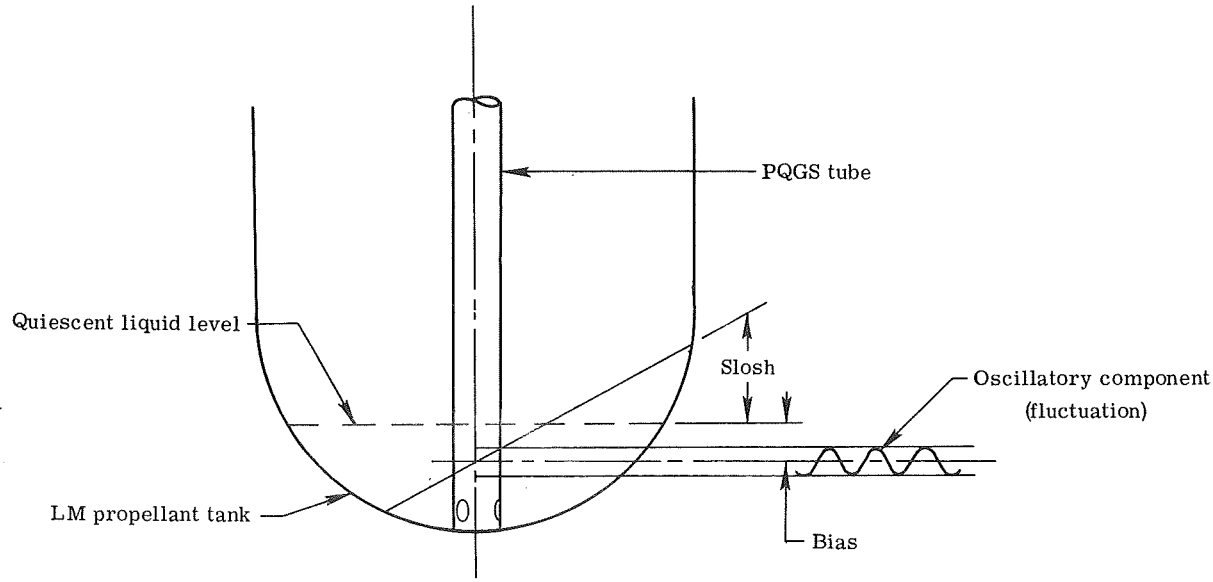

Figure 11.- PQGS tube fluctuation phenomena.

is comprised of two components: a steady component, or bias, and an oscillatory component centered about the bias level. Results showing the effect of the area of the vent holes on the oscillatory component are presented in this section. Other variations to the PQGS tube were investigated, and some of the results of these tests are presented in appendix B. Two antislosh baffle configurations for decreasing the bias level were studied with emphasis on baffle effectiveness and compatability with constraints associated with installation in the LM tanks. Results of tests with these candidate baffles are also presented in this section. Additionally, a potential problem in LM flight which was discovered in the higher amplitude tests was the uncovering of the zero-g can at high slosh amplitudes and low liquid levels. Results of tests related to this potential problem are discussed in appendix C.

Minimization of the Oscillatory Component of the PQGS Response

Data were collected during the manual excitation of the apparatus (fig. 4) and are presented as both fluctuation and bias as a function of slosh amplitude for quiescent liquid depths of 12.7 and 25.4 cm, which were the levels of interest. Lateral slosh amplitudes exceeding 25.4 cm were difficult to obtain at a liquid depth of 12.7 cm because of the presence of the antivortex baffle in the tank bottom, and data for these amplitudes are limited.

The total liquid response envelopes for PQGS tubes A and B with the liquid excited in its first antisymmetric mode are given in figures 12 and 13, respectively. The data show that in all cases the peak-to-peak liquid fluctuation about the bias in the PQGS increases with slosh amplitude. Comparing the vent-hole area of tube A with the vent-hole area of tube B shows a substantial reduction (approximately a factor of 4 at a slosh amplitude of 40.6 cm) of the liquid fluctuation in the tube for both depths tested. This reduction in fluctuation about the bias level reduced the premature low-level indicator penalty to approximately 19 seconds. As evidenced by the data, the bias is dependent upon slosh amplitude but is virtually independent of the tube configuration. On the basis of these results, the PQGS tubes in the existing Apollo LM tanks were immediately modified.

Also presented in figures 12 and 13 are results from a simulated "worst case" RCS lateral disturbance from the drop-weight slosh apparatus (fig. 4) on a quiescent liquid surface. First-cycle response results are those which were obtained in the PQGS during the first slosh cycle after the tank disturbance. Highest amplitude response data are given as the highest measured liquid response in the PQGS regardless of the cycle of slosh. It is important to note that both the first-cycle and highest amplitude response for tubes A and B at the 25.4-cm depth never exceeded the value for steady-state excitation. At the 12.7-cm depth, however, highest response value in all cases exceeded that value presented for steady-state excitation. Data obtained during the first slosh cycle of "worst case" input on an existing slosh condition, rather than on a quiescent surface, resulted in PQGS values which were less than those measured with input to a quiescent surface in all cases. This behavior resulted whether the input amplified or attenuated (in or out of phase) the existing slosh condition.

Minimization of Steady Component (Bias) of the PQGS Response

Tests involving the use of antislosh baffles were conducted to attempt to eliminate the inherent and significant time error in the PQGS due to bias (approximately 19 seconds fuel-burn time). Preliminary experiments were accomplished on a variety of antislosh baffles to examine methods of substantially decreasing or possibly eliminating the bias error. Basic baffle designs considered at that time included (1) a reticulated polyurethane foam mat, (2) a radial arm (solid and wire-mesh screen) pivoted about the PQGS tube,

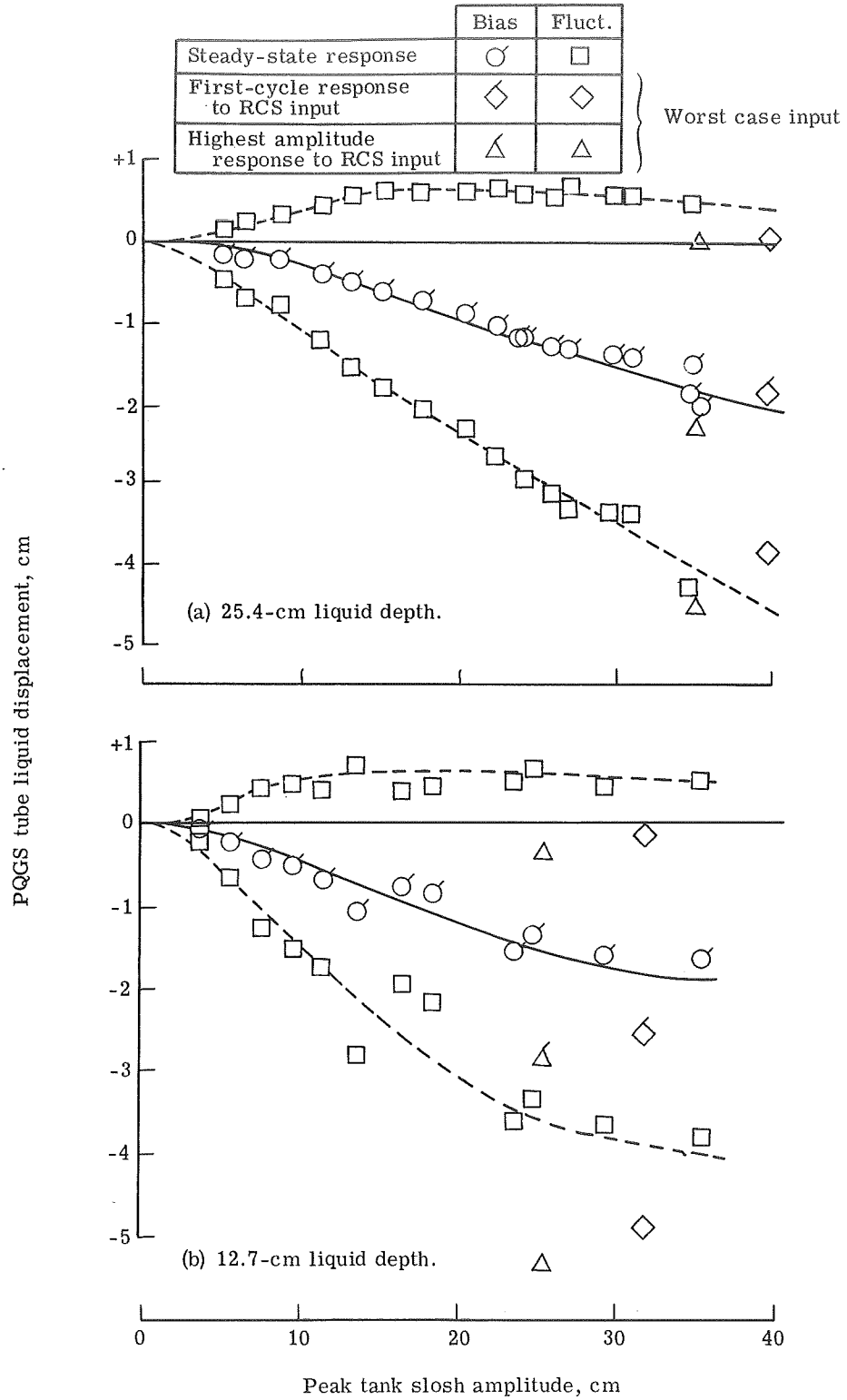

Figure 12.- Liquid response in PQGS tube A for first antisymmetric mode.

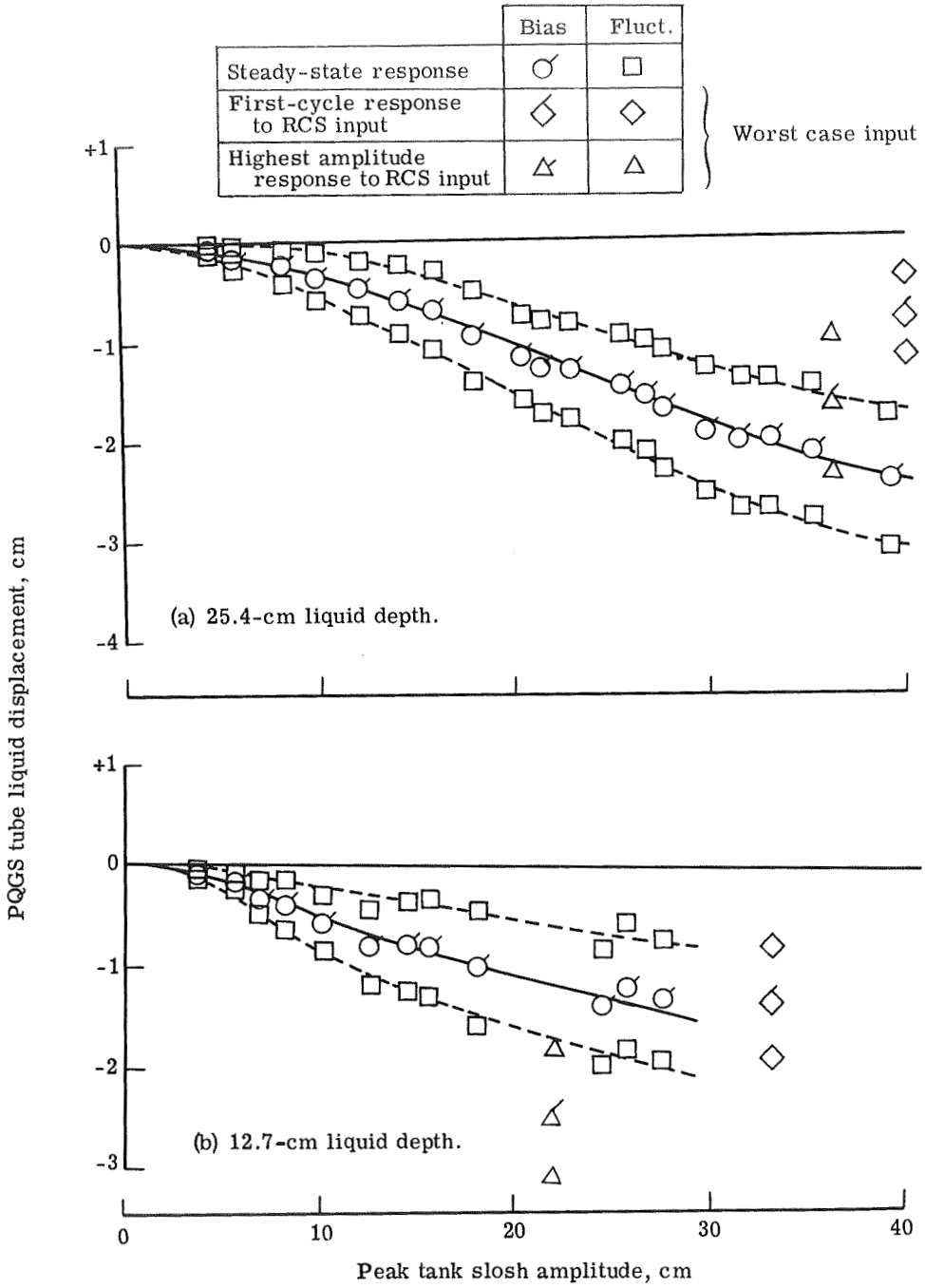

Figure 13.- Liquid response in PQGS tube B for first antisymmetric mode.

(3) lightweight, 5.7-cm-diameter, plastic perforated spherical shells (anchored and floating), (4) solid annular rings (single and multiple) attached to the tank wall, (5) a four-pointed "star" combined with either an unperforated or a perforated wall cylinder, and (6) a cylindrical baffle (wire-mesh screen, solid wall with external fins, and perforated wall with external fins). In evaluating these preliminary configurations, two very important constraints were considered: (1) Any device that was to be selected for use would have to be compatible with both the LM fuel and oxidizer (Aerozine-50 and N_2O_4, respectively), and (2) the device would have to be inserted into the LM tanks through an existing 6.1-cm-diameter access port to eliminate the requirement for new flight qualification tests on the tanks, which would be required if a new access hole were put through the tank wall. As a result of the preliminary evaluation, the four-pointed star baffle (fig. 14) and the cylindrical baffle (fig. 15) were selected for further experiments.

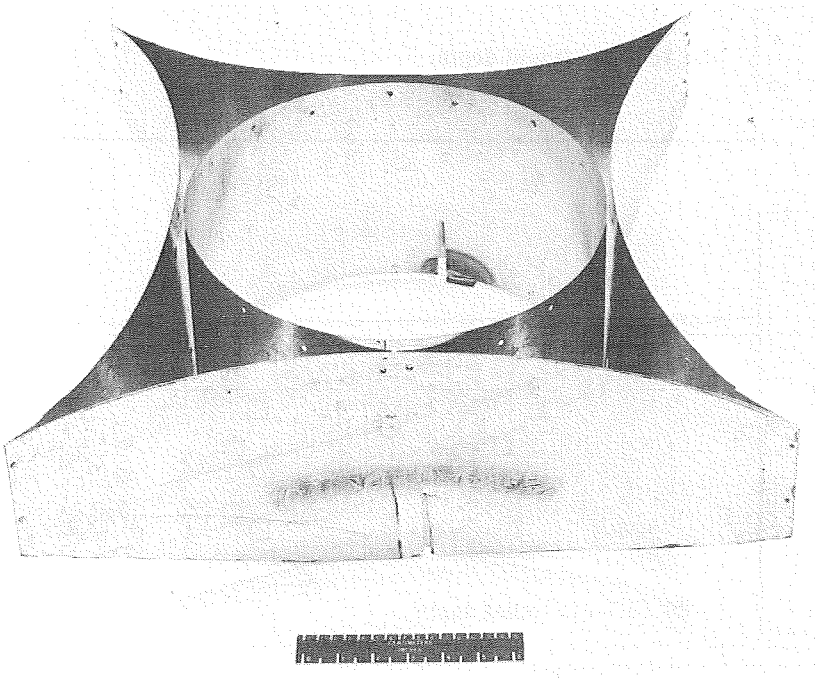

L-70-5747

(a) Solid-wall cylinder.

Figure 14.- Four-pointed star baffle.

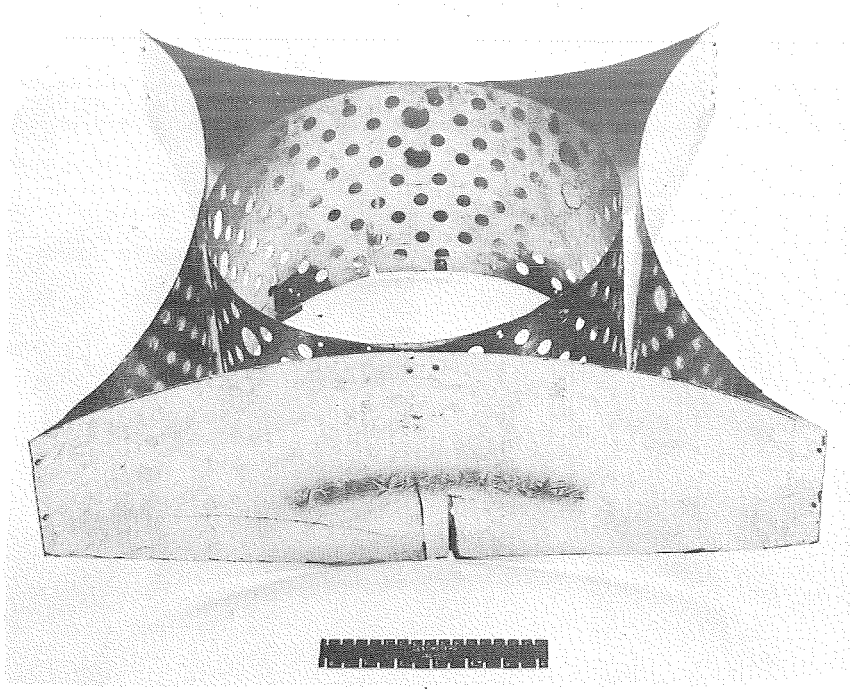

L-70-5748

(b) Perforated-wall cylinder.

Figure 14.- Concluded.

Data were obtained with the tank assembly installed in the drop-weight apparatus described in figure 4. Single worst case lateral disturbances simulating RCS pulses were imparted to the system with a liquid depth of 25.4 cm, and resulted in peak slosh amplitudes of 38.1 to 40.6 cm. Only tube B (0.5-cm-diameter vent holes) was used for the studies, since it had previously been selected as the replacement tube for the Apollo LM system.

The results of tests with the four-pointed star baffle and antivortex baffle are shown in figure 16. The data show a significant reduction in the bias level (in most cases, to the point of going above zero) when compared with the results for the antivortex baffle only. The bias is dependent upon direction of excitation when a perforated cylinder is used as the center ring but independent of slosh direction when an unperforated cylinder is used.

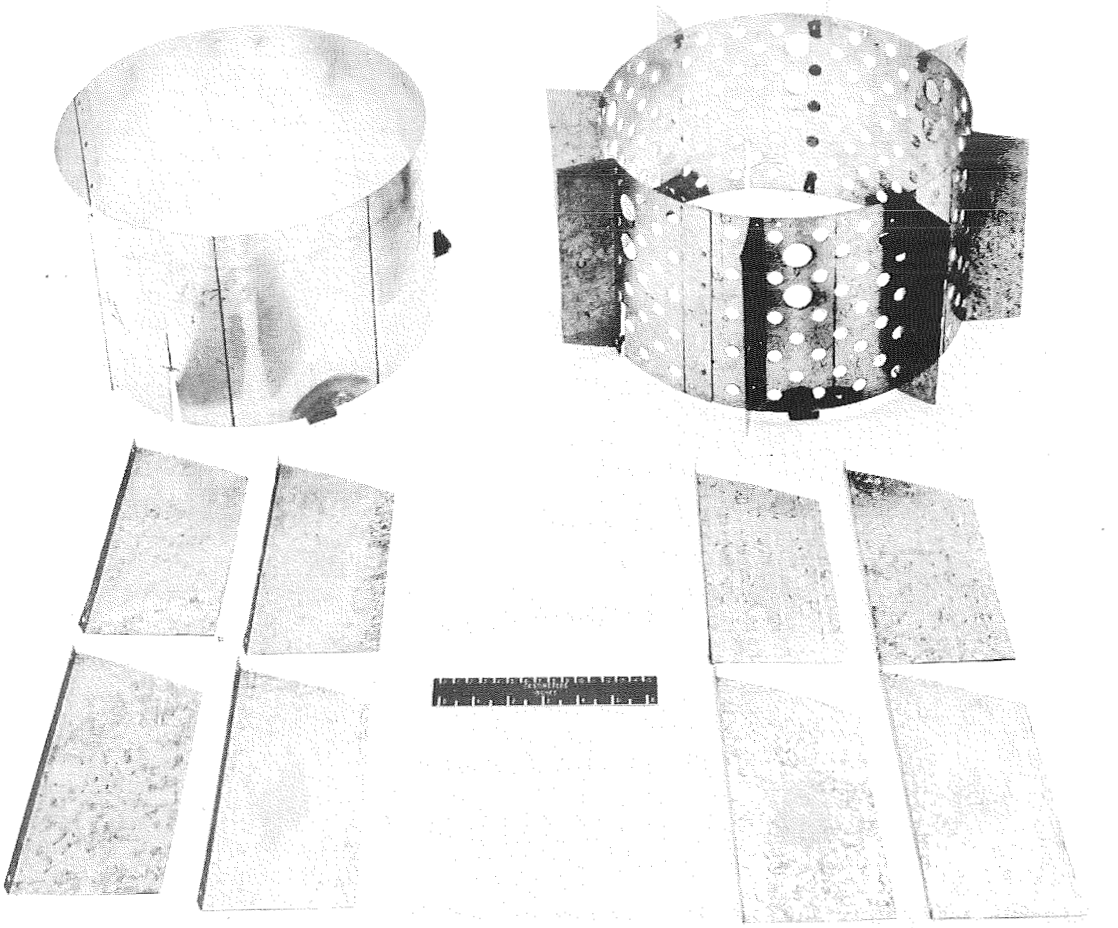

L-70-5746

Figure 15.- Cylindrical baffle.

Presented in figure 17 are the results from tests with a 20.3-cm-high perforated cylinder and antivortex baffle for various degrees of perforation. All test conditions showed a marked reduction in the bias level. As the data show, the bias was dependent upon percentage of open area, changing from minus to plus values as the percentage was decreased. For test condition E-2 (5 percent open area), the penalty for early low-level fuel indication was reduced to less than 5 seconds. Although test condition F-1 (9 percent open area, 10.2- by 20.3-cm solid fins) appeared to be a better "fix" than E-2, the increase in the size of the fins would impose added hardship during installation into the tank. It therefore appeared that the E-2 configuration would be a near-optimum baffle suitable for ready installation in the existing LM propellant tanks.

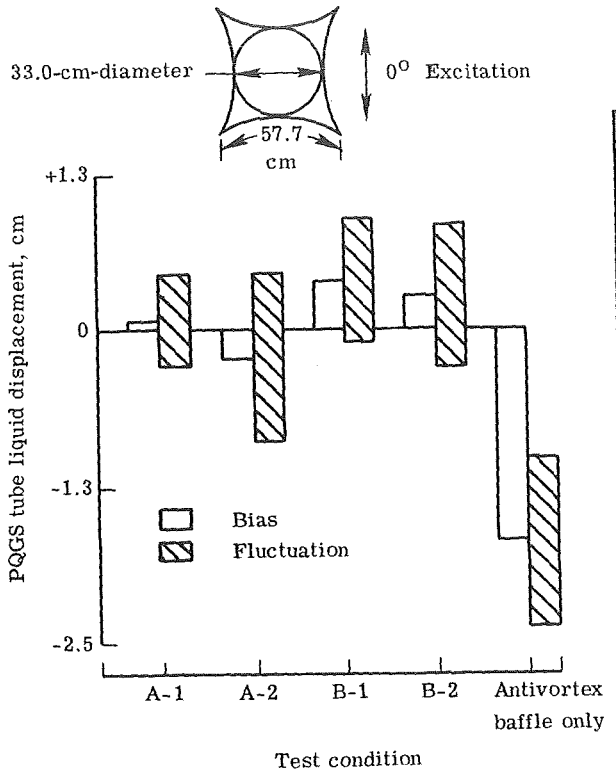

Test	Direction of excitation	Description
A-1 A-2	0° Rotated 45°	Star baffle with perforated cylinder plus antivortex baffle
B-1 B-2	0° Rotated 45°	Star baffle with unperforated cylinder plus antivortex baffle

Figure 16.- Liquid response in PQGS tube B with 20.3-cm-high star baffle at 25.4-cm liquid depth.

In order to install the 33.0-cm-diameter baffle through the 6.1-cm-diameter port, the baffle was constructed of a very resilient metal (a titanium alloy). The baffle was deformed by rolling it up into a compact cylinder which was then inserted through the port. After insertion, the baffle sprang back to its undeformed configuration for fastening to the antivortex baffle.

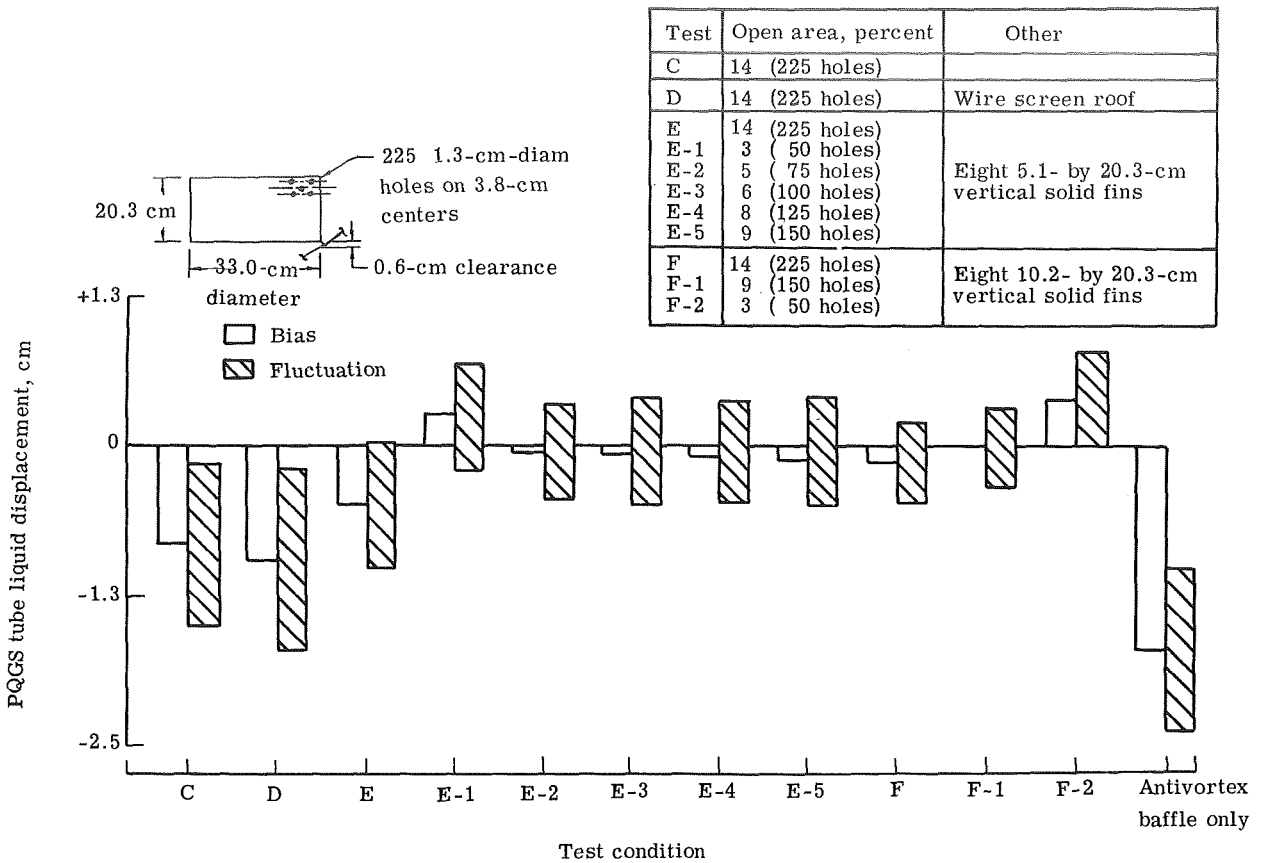

Test	Open area, percent	Other
C	14 (225 holes)	
D	14 (225 holes)	Wire screen roof
E	14 (225 holes)	Eight 5.1- by 20.3-cm vertical solid fins
E-1	3 (50 holes)	
E-2	5 (75 holes)	
E-3	6 (100 holes)	
E-4	8 (125 holes)	
E-5	9 (150 holes)	
F	14 (225 holes)	Eight 10.2- by 20.3-cm vertical solid fins
F-1	9 (150 holes)	
F-2	3 (50 holes)	

Figure 17.- Liquid response in PQGS tube B with 20.3-cm-high perforated cylinder and antivortex baffle at 25.4-cm liquid depth.

CONCLUDING REMARKS

Tests and supporting analyses were conducted to better understand and possibly eliminate a premature indication of a low level of propellant in the lunar module (LM) which occurred on both Apollo 11 and Apollo 12 missions. The problem was identified as being produced by liquid fluctuations in the propellant quantity gage system (PQGS) caused by sloshing within the LM fuel tank. These liquid fluctuations imposed an early warning penalty of approximately 30 to 45 seconds in the activation of the low-level indicator. The fluctuations within the tube are comprised of two parts, a steady component, or bias, and an oscillatory component centered around the bias.

The PQGS low-level indicator penalty was reduced to approximately 19 seconds during tests by decreasing the diameter of the PQGS vent holes to 0.5 cm. This decrease caused the oscillatory component of the fluctuation to be minimized consistent with constraints imposed by tank draining.

The installation of a 20.3-cm-high by 33.0-cm-diameter, thin-walled, slightly perforated cylindrical baffle, with eight 5.0- by 20.3-cm vertical solid fins reduced the bias during tests to a value at which the early low-level indicator penalty was less than 5 seconds at the nominal 25-cm liquid depth.

The two modifications (reduction of vent-hole diameter and installation of the baffle) were performed on the LM of Apollo 14, and analysis of flight data indicated that these modifications yielded a highly successful solution to the problem.

Langley Research Center,
National Aeronautics and Space Administration,
Hampton, Va., September 10, 1971.

APPENDIX A

LOW-LEVEL SINUSOIDAL DETERMINATION OF TANK PQGS SLOSH MODES

In an attempt to identify the slosh modes which could potentially cause large fluctuations in the PQGS, initial studies were conducted at low vibration levels. In this appendix the apparatus and test specimens used in these studies are described, results of the tests associated with the various modes are presented, and a comparison of calculated motion with measured motion in the PQGS when sloshing occurs in the most significant mode is shown.

Lateral sinusoidal excitation of constant acceleration magnitude was imparted to the tank by using the apparatus shown in figure 18. The 127.0-cm-diameter plexiglass

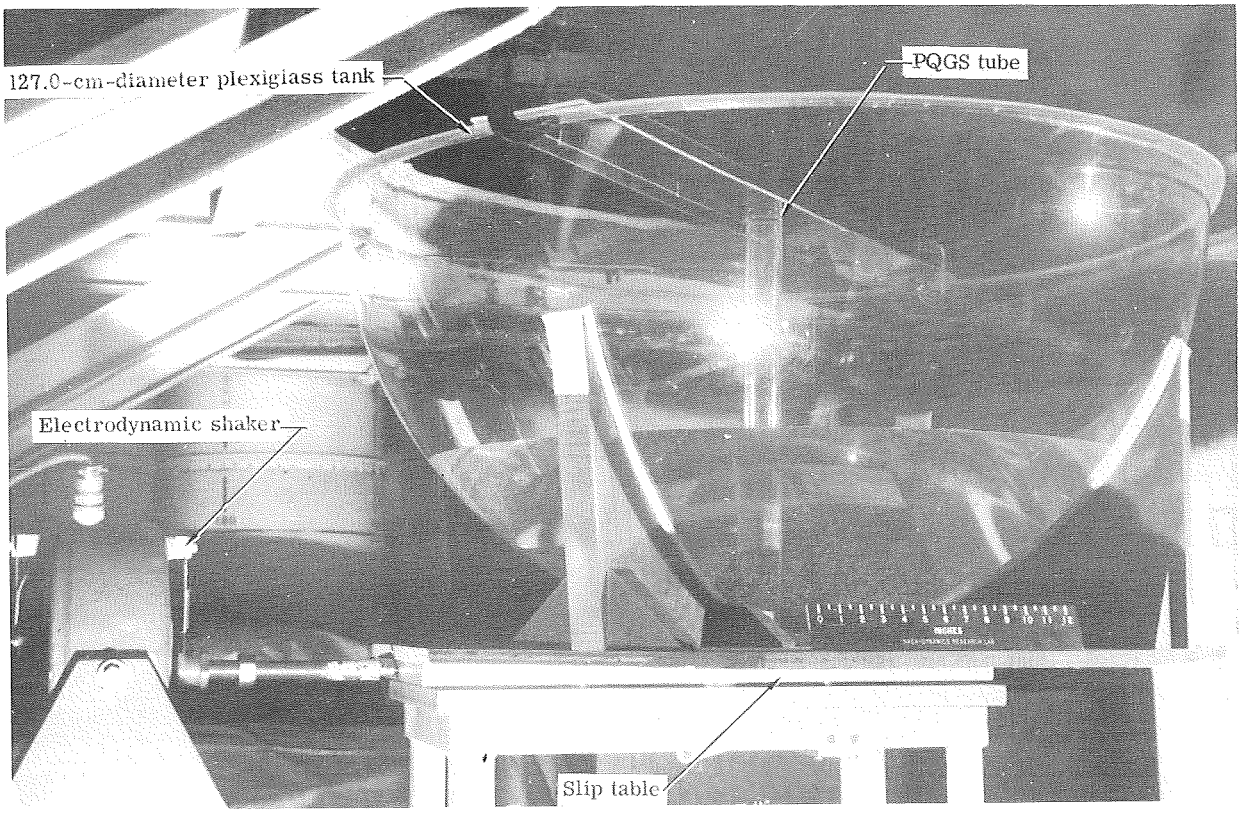

L-70-1970.1

Figure 18.- Lateral-excitation apparatus.

tank, supported by a wood cradle, was placed atop a slip table, and PQGS tube C (identical to PQGS tube A except there were no rivet mandrel holes) was installed in the tank, which was filled with water to a depth of 25.4 cm. The tank was then driven laterally by an electrodynamic shaker. With the tank acceleration amplitude held constant, the frequency

of excitation was slowly increased from 0 to 1.4 Hz. As shown in figure 19, tank slosh response and related PQGS oscillations were observed at several frequencies. (Schematic

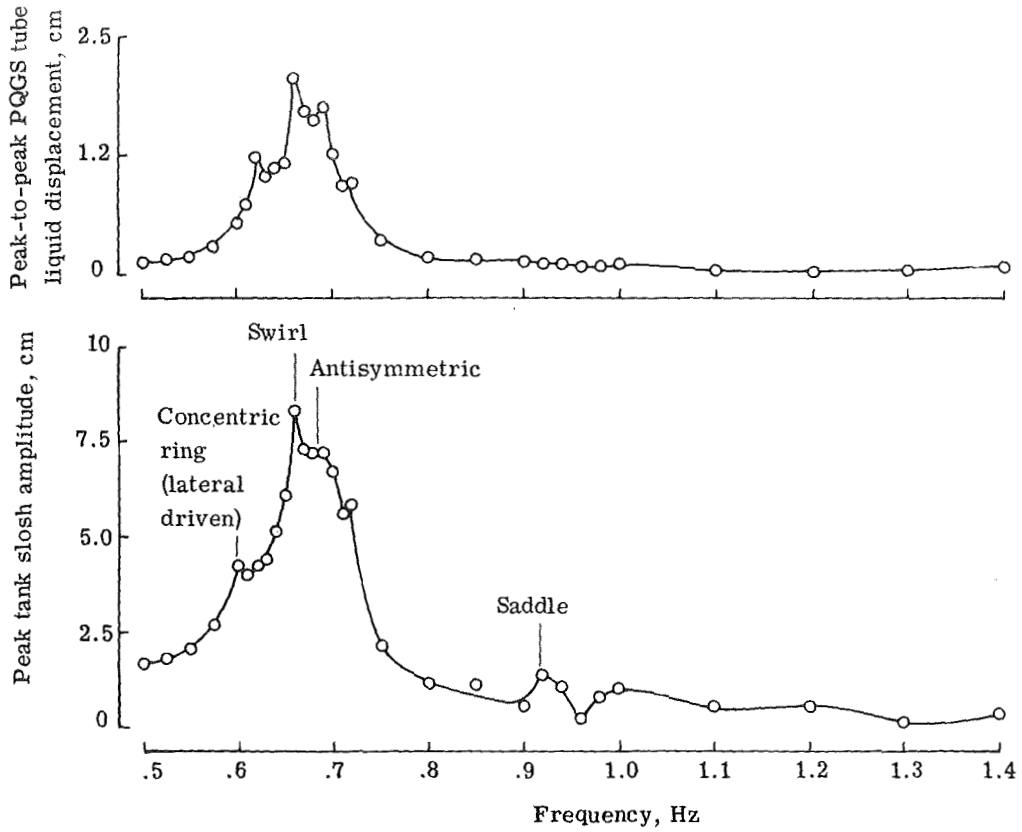

Figure 19.- Liquid response to frequency sweep for constant lateral vibratory acceleration.

diagrams of the principal slosh modes (ref. 7) are shown in figure 20, and their measured frequencies for several liquid levels are presented in table II.) As the frequency increased from zero, the liquid in the tank exhibited relatively low-level lateral motion at the driving frequency. When the sweep frequency was nearly equal to one-half the frequency of the concentric-ring mode (0.59 Hz) (ref. 8), a combined lateral—concentric-ring mode of relatively low amplitude was observed. There was little associated PQGS liquid motion at this frequency. However, as the frequency was further increased to 0.68 Hz, a marked resonance occurred in the fundamental antisymmetric lateral mode, at which time the associated peak PQGS response was measured. At a driving frequency near that of the fundamental lateral mode (0.65 Hz), low-amplitude swirl could be induced by "fine tuning." Even though there was a marked increase in the PQGS liquid response at this frequency, the tank slosh could only be excited by applying a constant frequency-amplitude relationship for a long period of time. It is unlikely that this combination would be encountered and/or maintained during LM flight. The only other mode of significance

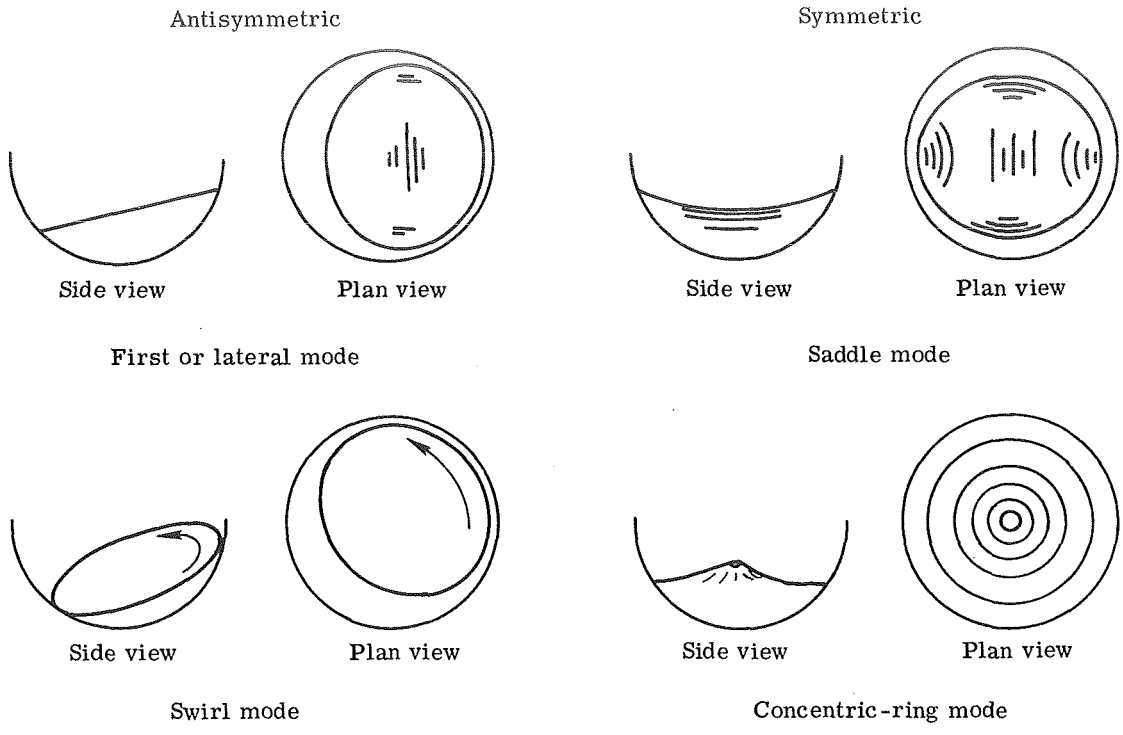

Figure 20.- Principal slosh modes.

was the saddle mode (approximately 0.91 Hz); however, this mode had very little related PQGS liquid motion. The test was repeated with tube D (identical to PQGS tube B except that there were no rivet mandrel holes) and it was found that the above results did not vary for the smaller liquid vent orifices.

Although the concentric-ring mode was not easily excited by lateral motion, upon removal of the excitation, the liquid would often decay in the concentric-ring mode because of low damping in comparison with the lateral mode. Therefore, the concentric-ring mode (1.20 Hz) was studied in more detail by applying a vertical excitation to the liquid by use of the apparatus shown in figure 21. The tank was placed atop a hydraulic shaker and supported from above by soft springs (four 1.3-cm-diameter bungee cords). Tube C and other associated equipment were placed in the tank, which was filled with water to a depth of 25.4 cm. The tank was then excited vertically at the frequency of the concentric-ring mode, which required fine tuning of the driving frequency, high-amplitude input, and long periods of excitation time. For example, a time period of approximately 20 seconds at an amplitude of 1.3 cm peak to peak was required to induce the concentric-ring mode. In addition, the control frequency mode of the LM was not within the frequency range of the concentric-ring mode. It was therefore concluded that it would be very difficult to excite these combinations of inputs simultaneously on the Apollo LM flight system.

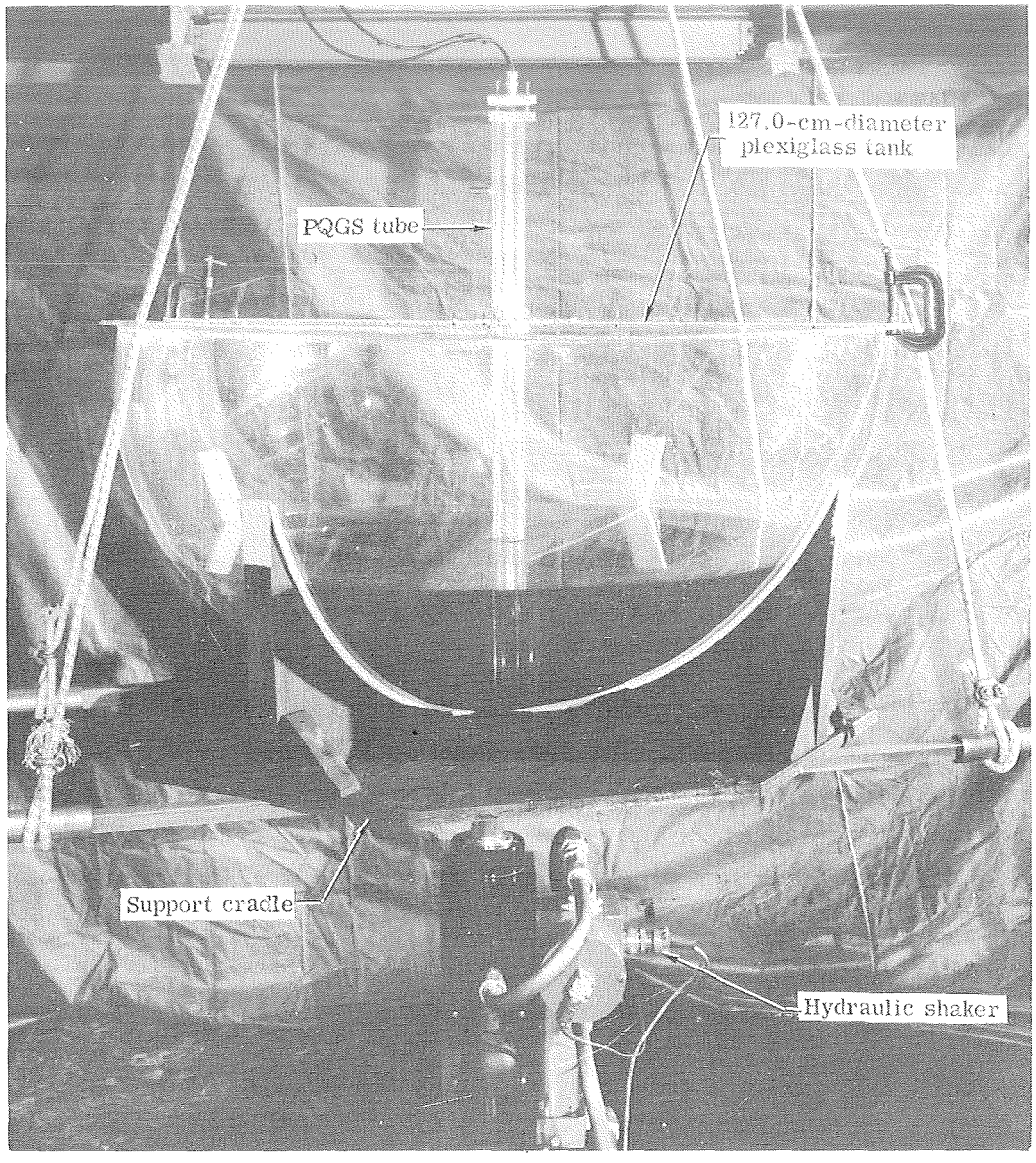

L-70-3518.1

Figure 21.- Vertical-excitation apparatus.

Results of the tests and analysis are presented in figure 22. The maximum sloshing amplitude used in the test-analysis comparison was 12.7 cm. The slosh mode was assumed to be the fundamental antisymmetric lateral (0.68 Hz) mode. Comparisons made at higher amplitudes become invalid principally because the surface of the liquid in the tank, which was assumed to be a plane in the analysis, becomes distorted. The figure shows the total displacement of the liquid in the PQGS tube as a function of the slosh amplitude. Results are shown for both tubes C and D. Analytically, the bias (dashed line) is the same for both tubes. Four solid lines are shown which indicate the calculated amplitude of the fluctuation relative to the bias. The agreement between the predicted

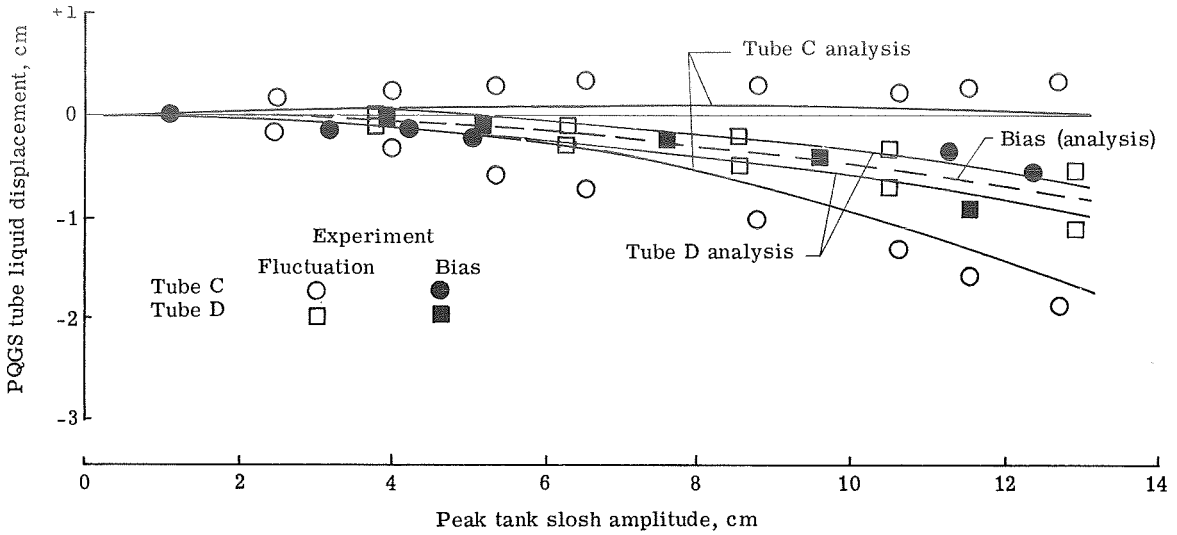

Figure 22.- Experimental and analytical comparison of liquid response in PQGS tubes C and D for antisymmetric mode at 25.4-cm liquid depth.

and measured trends is considered good. In general, the analysis underestimates the amplitude of the fluctuation slightly. The agreement could be improved by altering the assumed orifice discharge coefficient, but it was felt that such changes would be somewhat arbitrary and unwarranted. On the basis of these results, the analysis was thought to have accomplished its objective of assuring an understanding of the PQGS liquid dynamics.

APPENDIX B

PQGS VARIATIONS

A variety of PQGS tube configurations were investigated to find the effect of vertical vent-hole spacing, multiple vent holes, and flow deflectors on the liquid fluctuation and, in particular, the liquid bias within the tube. The apparatus shown in figure 18 was used for the tests. All associated test equipment was placed in the tank, which was then filled to a depth of 25.4 cm. An electrodynamic shaker drove the tank sinusoidally in the lateral direction atop a slip table at the frequency of the fundamental antisymmetric slosh mode. Slosh amplitudes from 0 to 20.3 cm were achieved by this method.

Effect of Multiple-Vent Holes

The three multiple-vent-hole configurations are shown in figure 23. The total vent-hole area for each tube was constant. The results of the tests are presented in figure 24.

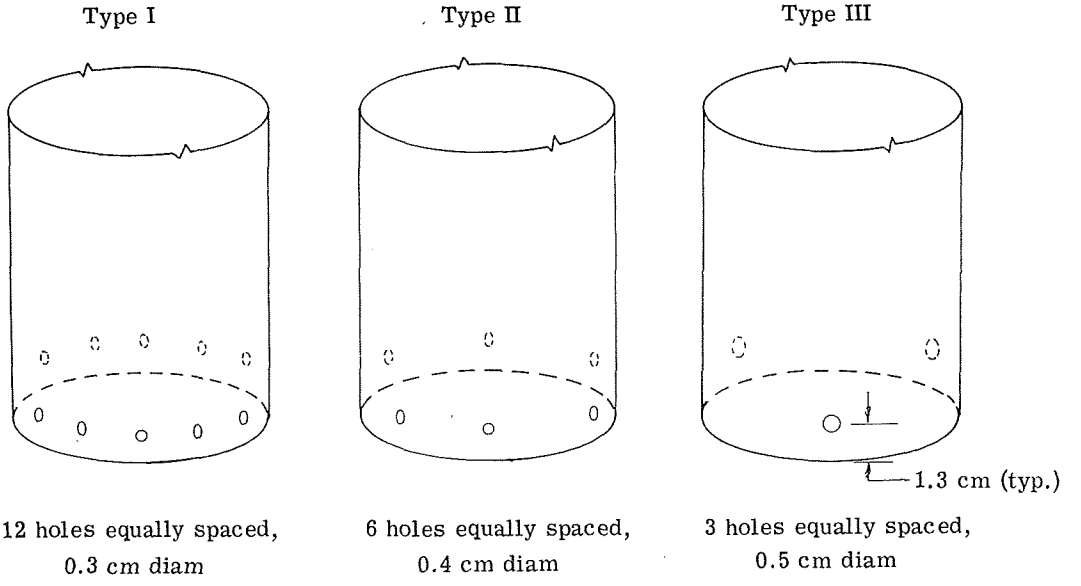

Figure 23.- PQGS tube with variations in number of vent holes.

No significant change was apparent in the data for either tube fluctuation or tube bias as a result of either three, six, or 12 vent holes when compared with PQGS tube D (three 0.5-cm-diameter vent holes 1.3 cm above the base).

Effect of Hole Orientation

The type IV tube (fig. 25) was used to study the effect of vent-hole orientation. The results are presented in figure 26. Note that the direction of the flag on each symbol

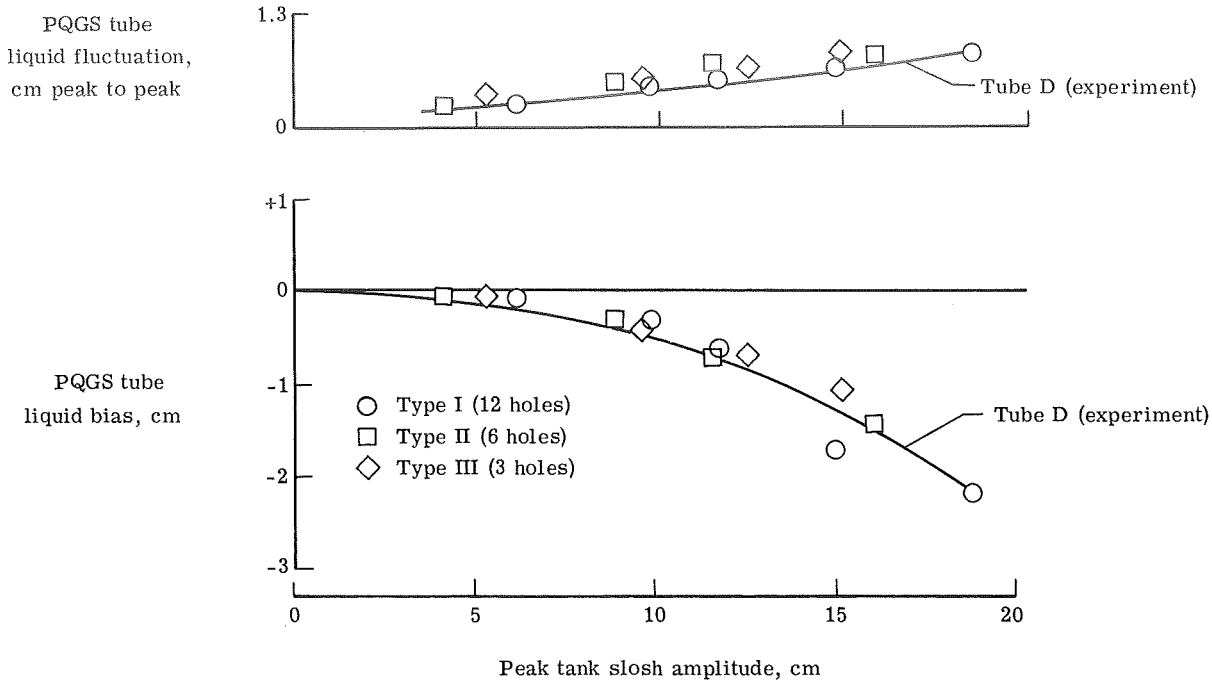

Figure 24.- Effect of multiple vent holes on PQGS liquid response for antisymmetric mode at 25.4-cm depth.

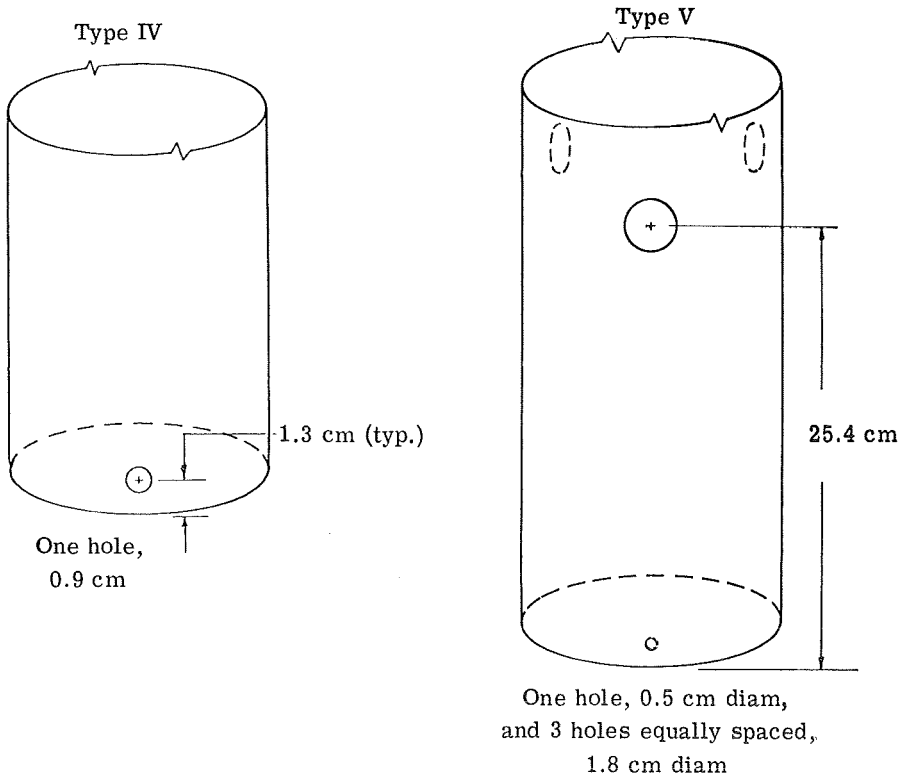

Figure 25.- PQGS tube with variations in vent-hole spacing and orientation.

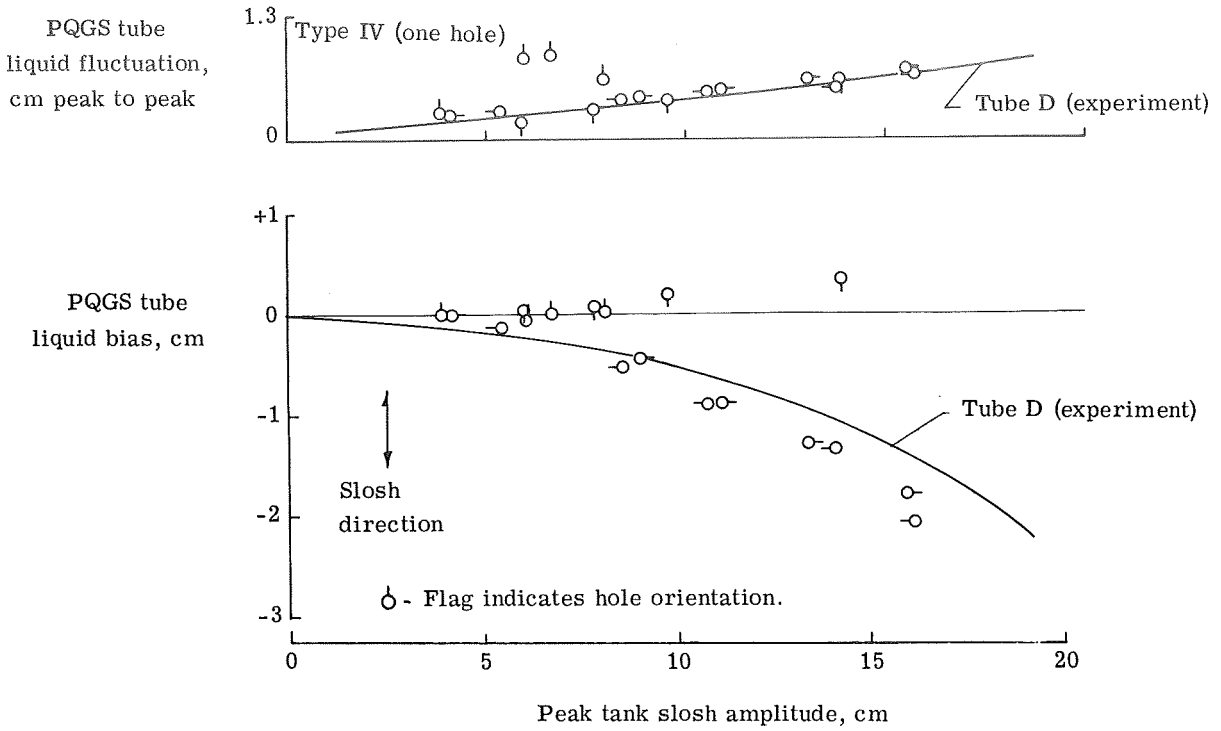

Figure 26.- Effect of vent-hole orientation on PQGS liquid response for antisymmetric mode at 25.4-cm depth.

indicates hole orientation. The fluctuation within the tube was not greatly affected by orienting the vent-hole axis perpendicular to the direction of excitation when compared with tube D. However, when the vent-hole axis was oriented parallel to the direction of excitation, an increase in the fluctuation is apparent at slosh amplitudes near 6 cm. For tube bias, however, it can be seen that when the vent hole was placed parallel to the liquid slosh, there was a significant decrease to the point that it surpassed the quiescent level (zero) for slosh amplitudes greater than 10.2 cm. When the hole was placed perpendicular to the direction of slosh, there was little change in the liquid bias.

Effect of Vertical Hole Spacing

Tests with the type V tube (fig. 25) produced results presented in figure 27. As evidenced by the data, there appeared to be little effect on fluctuation of spacing the three vent holes 25.4 cm from the base of the tube when compared with PQGS tube C (1.8-cm-diameter vent holes) where holes were 1.3 cm from the bottom. However, the tube liquid bias was significantly affected and went from below to above the quiescent or zero level for slosh amplitudes greater than 10.2 cm.

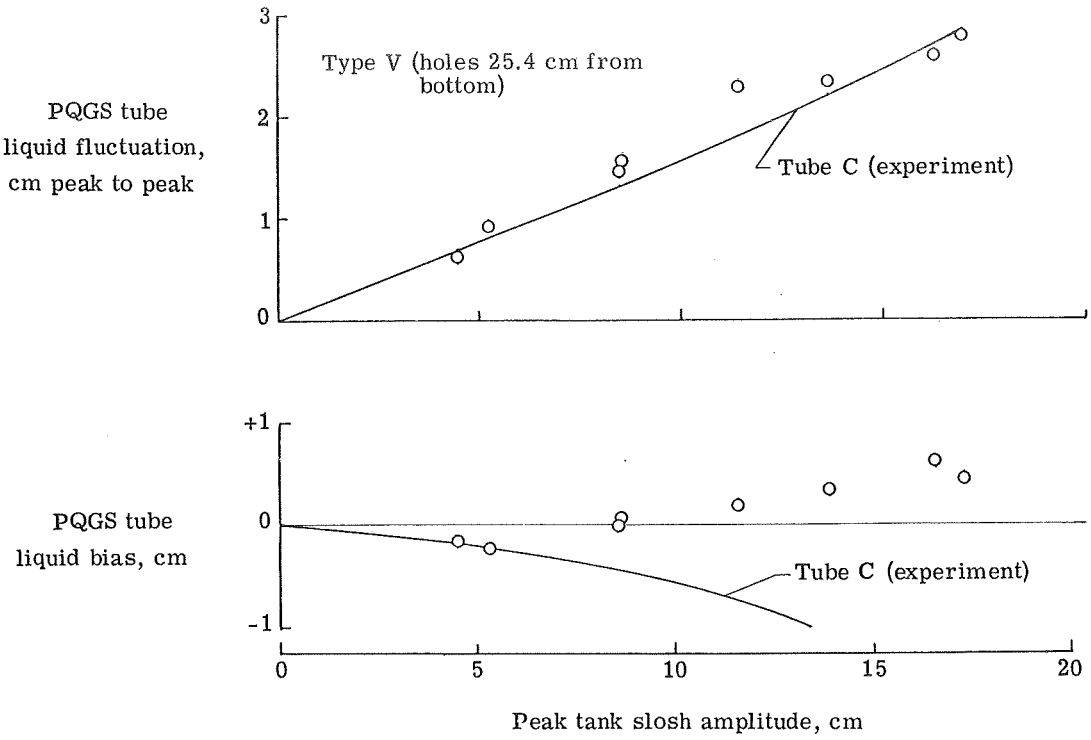

Figure 27.- Effect of vertical vent-hole spacing on PQGS liquid response for antisymmetric mode at 25.4-cm depth.

Effect of Flow Deflectors

Figure 28 shows the four vent-hole deflector configurations tested. The results of these tests are presented in figure 29. Tube C data without deflectors are included for reference, and, as can be observed from the data, none of the deflectors provided any substantial reductions of the liquid fluctuation or bias, except perhaps type IX (solid can).

It was concluded from the overall evaluation of the tests that little improvement in the reduction of the PQGS fluctuation and bias was gained by the use of vent-hole deflectors, orientation, or spacing, or multiple vent holes.

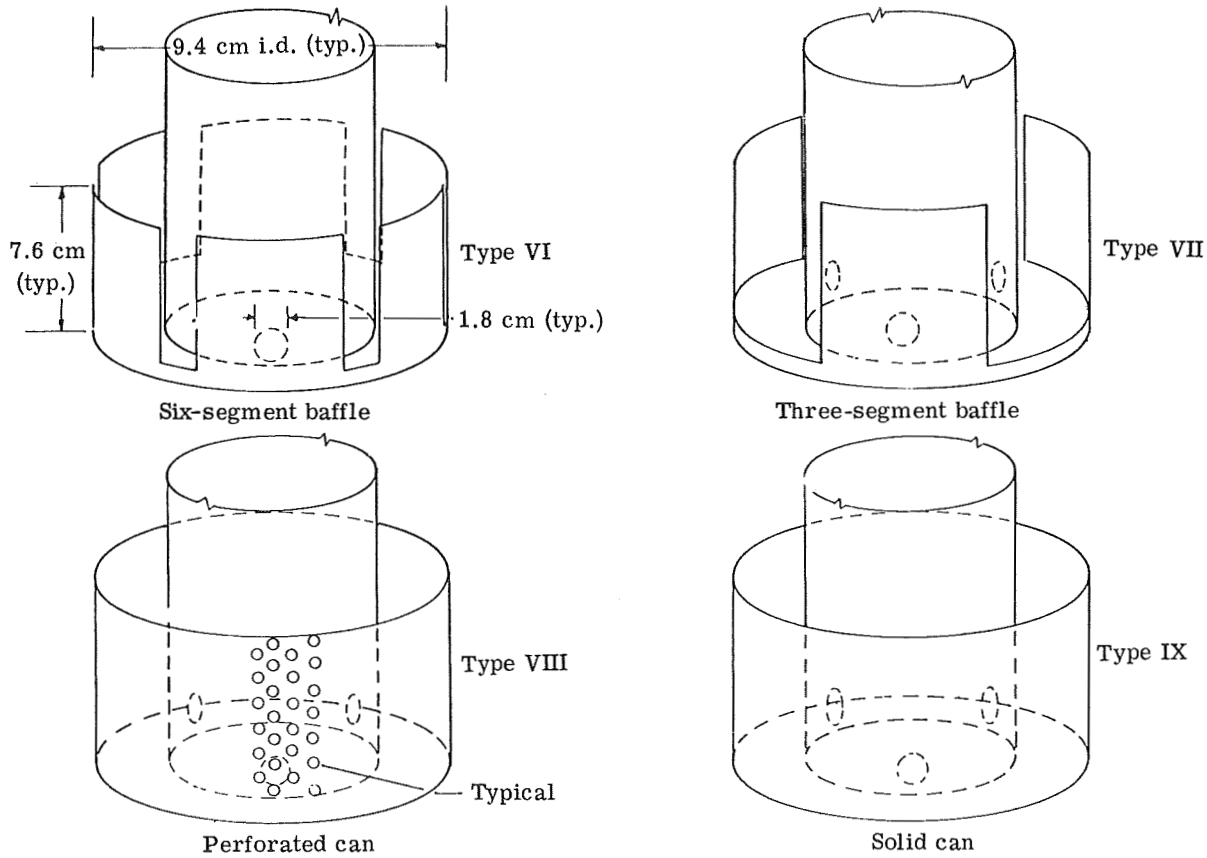

Figure 28.- PQGS tube with variations in vent-hole deflectors.

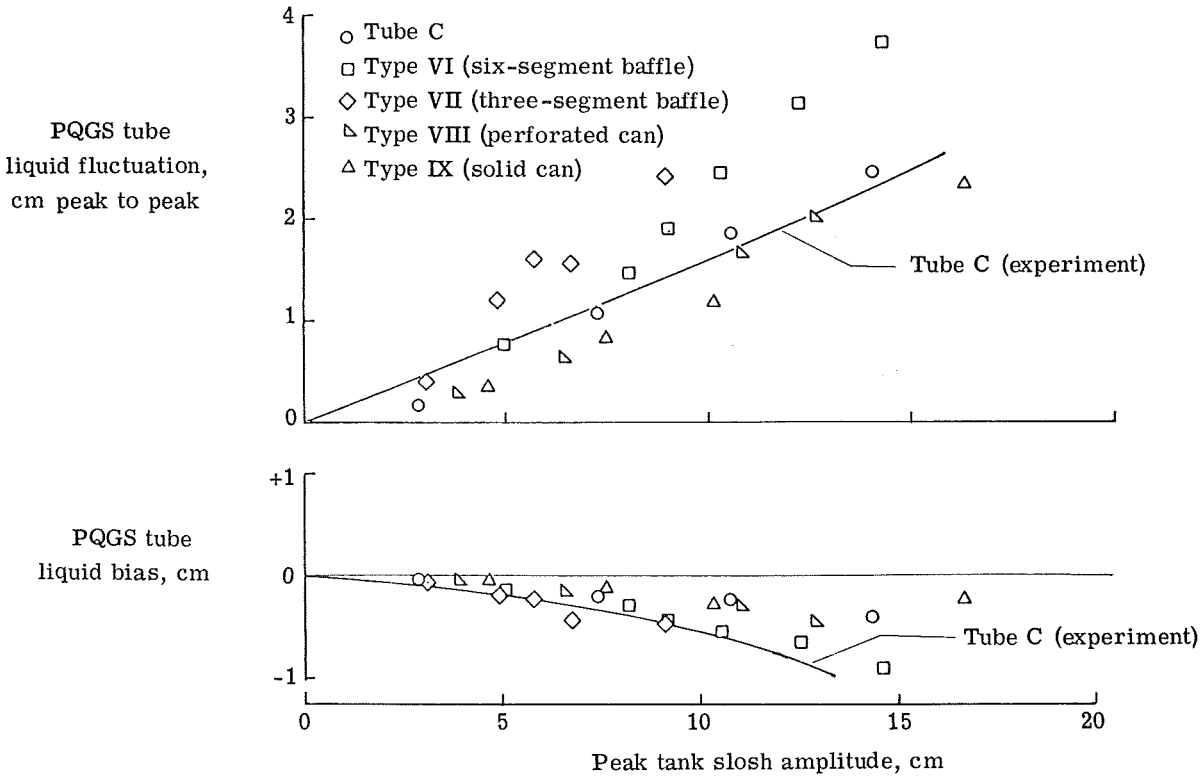

Figure 29.- Effect of vent-hole deflectors on PQGS liquid response for antisymmetric mode at 25.4-cm depth.

APPENDIX C

TANK DRAINING WHILE SLOSHING

During tests to minimize the oscillatory component (fluctuation) within the PQGS, it was apparent that when the liquid was at the 12.7-cm depth in the tank, the zero-g can became uncovered during a typical worst case RCS disturbance. This "unporting" of the zero-g can could lead to serious consequences should the can ever be void of fuel during a "power on" phase of the Apollo flight. Studies were therefore carried out to determine whether gaseous entrainment occurred in the tank effluent during sloshing and draining at low liquid levels.

Complete results of the LM tank drain tests are documented in a supplementary film (L-1088). The film records indicate that for a liquid depth of 12.7 cm and 0.12-m^3/min flow (hover) condition, unporting of the zero-g can occurred during the first wave cycle following a lateral acceleration of ±0.2g for a period of 0.4 second. For liquid depths of 15.2 and 17.8 cm, unporting did not develop during the first wave cycle, but air trapped by the severe liquid turbulence did become entrained in the tank effluent during later wave cycles. No unporting was evident during "full throttle" (0.23 m^3/min) tests where the acceleration and/or force input was ±0.05g for a duration of 0.9 second. This simulated RCS input was selected to be less than that associated with the hover tests because during full thrust the RCS input will have less effect on the liquid which is in a system experiencing greater gravitational force.

REFERENCES

1. Rimer, M.; and Stephens, D. G.: The Effect of Liquid Oscillations on the LM Propellant Quantity Gauge System. Shock Vib. Bull. 41, Pt. 7, U.S. Dep. Def., Dec. 1970, pp. 181-194.

2. Hunsaker, J. C.; and Rightmire, B. G.: Engineering Applications of Fluid Mechanics. McGraw-Hill Book Co., Inc., 1947.

3. Schiller, L.; and Linke, W.: Pressure and Frictional Resistance of a Cylinder at Reynolds Numbers 5,000 to 40,000. NACA TM 715, 1933.

4. Anon.: Slosh Suppression. NASA Space Vehicle Design Criteria (Structures). NASA SP-8031, 1969.

5. Stephens, David G.; Leonard, H. Wayne; and Perry, Tom W.: Investigation of the Damping of Liquids in Right-Circular Cylindrical Tanks, Including the Effects of a Time-Variant Liquid Depth. NASA TN D-1367, 1962.

6. Stephens, David G.; and Scholl, Harland F.: Effectiveness of Flexible and Rigid Ring Baffles for Damping Liquid Oscillations in Large-Scale Cylindrical Tanks. NASA TN D-3878, 1967.

7. Pulgrano, L.; Low, R.; and Zentgraf, J. K.: Summary Report on the Study of Liquid Sloshing in the LEM Main Propellant Tanks. Rep. No. LED-520-10, Grumman Aircraft Eng. Corp., Jan. 10, 1966.

8. Abramson, H. Norman, ed.: The Dynamic Behavior of Liquids in Moving Containers. NASA SP-106, 1966.

TABLE I.- TEST PROGRAM

[Drop-weight apparatus; first antisymmetric slosh mode; test liquid water]

Input type	Liquid depth, cm	Baffle type	PQGS tube
Steady state, RCS pulse, and decay	12.7 and 25.4	Antivortex only	A and B
RCS pulse and decay	25.4	Four-pointed star or cylindrical with antivortex	B

TABLE II.- MEASURED FREQUENCY (Hz) IN 127.0-cm-DIAMETER TANK

Liquid depth, cm	Frequency, Hz, for –					
	Concentric-ring mode (lateral driven)	Swirl mode	Lateral antisymmetric mode	Saddle mode (driven)	Saddle mode (free)	Concentric-ring mode (free)
30.5	0.58	---	0.68	0.91	0.93	1.20
25.4	.59	0.65	.68	.91	---	1.20
22.9	.61	.66	.67	.92	---	1.20
17.8	.61	.64	.69	.90	.90	1.20
12.7	.62	---	.70	.89	.89	1.23

A motion-picture film supplement L-1088 is available on loan. Requests will be filled in the order received. You will be notified of the approximate date scheduled.

The film (16 mm, 5.5 min, color, silent) briefly shows the apparatus and techniques used to accomplish the various experiments described in the text, with emphasis on lunar module tank sloshing while draining.

Film supplement L-1088 is available on request to:

NASA Langley Research Center
Att: Photographic Branch, Mail Stop 171
Hampton, Va. 23365

Date _____

Please send, on loan, copy of film supplement L-1088 to TM X-2362.

_____
Name of organization

_____
Street number

_____
City and State Zip code

Attention: Mr. _____
Title _____

CUT

Place
Stamp
Here

NASA Langley Research Center
Att: Photographic Branch, Mail Stop 171
Hampton, Va. 23365

NATIONAL AERONAUTICS AND SPACE ADMISTRATION
WASHINGTON, D.C. 20546

OFFICIAL BUSINESS
PENALTY FOR PRIVATE USE $300

FIRST CLASS MAIL

POSTAGE AND FEES PAID
NATIONAL AERONAUTICS AND
SPACE ADMINISTRATION

U.S.MAIL

POSTMASTER: If Undeliverable (Section 158 Postal Manual) Do Not Return

"The aeronautical and space activities of the United States shall be conducted so as to contribute . . . to the expansion of human knowledge of phenomena in the atmosphere and space. The Administration shall provide for the widest practicable and appropriate dissemination of information concerning its activities and the results thereof."

— NATIONAL AERONAUTICS AND SPACE ACT OF 1958

NASA SCIENTIFIC AND TECHNICAL PUBLICATIONS

TECHNICAL REPORTS: Scientific and technical information considered important, complete, and a lasting contribution to existing knowledge.

TECHNICAL NOTES: Information less broad in scope but nevertheless of importance as a contribution to existing knowledge.

TECHNICAL MEMORANDUMS: Information receiving limited distribution because of preliminary data, security classification, or other reasons.

CONTRACTOR REPORTS: Scientific and technical information generated under a NASA contract or grant and considered an important contribution to existing knowledge.

TECHNICAL TRANSLATIONS: Information published in a foreign language considered to merit NASA distribution in English.

SPECIAL PUBLICATIONS: Information derived from or of value to NASA activities. Publications include conference proceedings, monographs, data compilations, handbooks, sourcebooks, and special bibliographies.

TECHNOLOGY UTILIZATION PUBLICATIONS: Information on technology used by NASA that may be of particular interest in commercial and other non-aerospace applications. Publications include Tech Briefs, Technology Utilization Reports and Technology Surveys.

Details on the availability of these publications may be obtained from:

SCIENTIFIC AND TECHNICAL INFORMATION OFFICE

NATIONAL AERONAUTICS AND SPACE ADMINISTRATION

Washington, D.C. 20546